‘Halo-kinematic’ sequence-stratigraphic analysis of minibasins in the deepwater contractional province of the Liguro-Provençal Basin, Western Mediterranean

V. Mianaekere*; J. Adam

Earth Sciences department, Royal Holloway university of London

**Corresponding author: victoria.mianaekere.2014@live.rhul.ac.uk,*

Abstract

This study investigates the co-evolution of gravity-driven thin-skinned salt tectonic processes and minibasin-scale halokinetic-depositional sequences for the kinematic analysis of salt diapirs in the diapiric province of the contractional domain of the deepwater Liguro-Provençal Basin. We apply minibasin-scale halo-kinematic sequence-stratigraphic concepts to investigate local controls of diapir growth and creation of accommodation space in related salt-withdrawal minibasins. Halokinetic wheeler diagrams extrapolated from 2D interpretation of geo-seismic sections show local temporal halokinetic processes of periods of ponding and nature of near diapir erosion or slumping. Structurally restored 2D minibasins along with derived structural wheeler diagrams, show the syn-kinematic cycle of events consisting of ponding, flap folding and erosion within minibasin sequences. Structural wheeler diagram demonstrates the transition from large length scale (100s of meters to several kilometers) folding above diapir pedestals to small length scale (10s of meters) folding proximal to steep diapir flanks. Large length scale folds are associated with early pre-kinematic layers; they mechanically rotate from minibasin center. Small length scale folds are associated with younger depositional sequences; they rotate from local depocentre focus points.

Keywords: Halo-kinematic sequence stratigraphy, minibasins, minibasin depositional patterns, salt tectonics, Messinian salt.

1. Introduction

This study investigates the co-evolution of passive margin gravity-driven thin-skinned salt tectonic processes and minibasin-scale salt tectonics in the diapiric province of the contractional domain of the deepwater Liguro-Provençal basin (Mianaekere and Adam 2020). Salt tectonics in the west Mediterranean evolved from a gravitational salt system with an up-dip extensional domain and a down-dip combined contractional-halokinetic minibasin domain (dos Reis et al. 2005; Leroux et al. 2015; Mianaekere and Adam 2020). Distribution of primary minibasins of a linked thin-skinned gravity-driven salt system and different magnitudes of regional contraction controlled by degree of margin tilt >1° is shown in (Fig. 1).

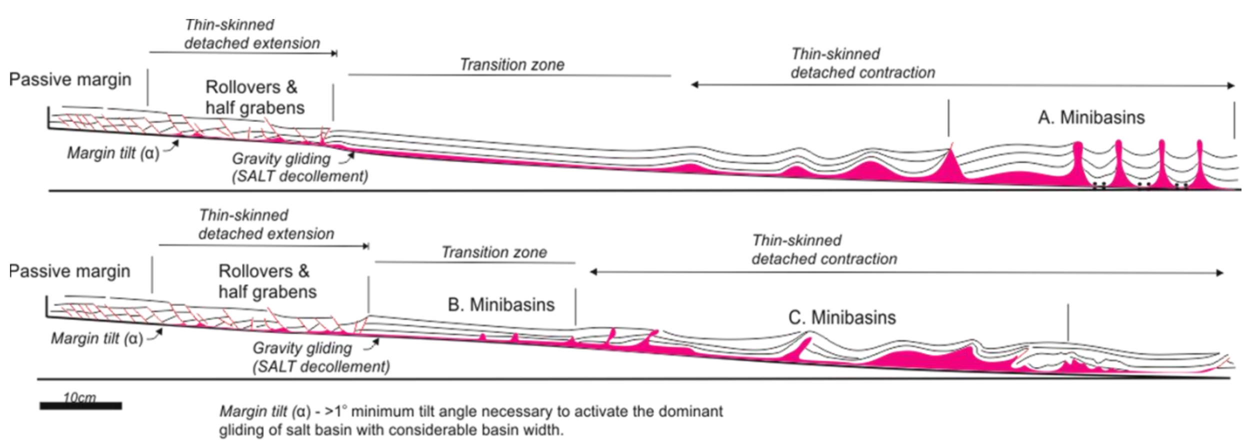

Figure 1: Salt tectonic styles on passive margins (Modified from Brun and Fort 2011). Note distribution of primary minibasins labelled A, B and C.

Figure 1 (a) Shows minibasins (A) formed in the contractional domain associated with passive down-building and regional squeezing or shortening. Minibasins (A) bound by vertical salt stocks may range in geometry from symmetrical to asymmetrical to rotated minibasins. Figure 1 (b) shows minibasins (B) formed in transitional zone, associated with passive downbuilding and minibasins (C) formed in the contractional domain associated with folding and thrusting. [see also (Brun and Fort 2011b; Brun and Fort 2010; Rowan et al. 2004; Rowan et al. 2012b) Minibasins (A) formed under low deformation rates and moderate total shortening is typical of the contractional domain of the deepwater Liguro-Provençal basin (dos Reis et al. 2005; Leroux et al. 2015; Mianaekere and Adam 2020).

Geo-dynamic history of study area

The NW Mediterranean north Balearic and Liguro-Provençal Cenozoic sedimentary basins (Fig. 2) developed during the NW-SE directed rifting and back-arc extension in Miocene times (Granado et al. 2016; Gunnell et al. 2008). The SE to late SSE rotational drift of the Corsica-Sardinia block and contemporaneous back-arc extension led to the early formation of a highly stretched continental crust and the late formation of the Miocene (21-16 Ma) oceanic crust beneath the Liguro-Provençal basin (Carminati et al. 2004; Maillard et al. 2003; Storetvedt 1973). Evaporites was extensively deposited on paleo Messinian basin above extended continental crust and oceanic crust during the pronounced late Miocene glacio-eustatic sea level regression (Butler et al. 1999; Droz et al. 2006) (Fig. 2). Post-Messinian isostatic adjustments of the continental shelves relative to the basin plain influenced prograding sedimentary wedges, gravitational failure and gravity-driven thin-skinned deformation, hence extensive salt diapirism is situated in the down-dip contractional domain in the deepwater basin overlying oceanic crust (Bonnel et al. 2005; dos Reis et al. 2005; Granado et al. 2016; Leroux et al. 2015; Maillard et al. 2003; Mianaekere and Adam 2020).

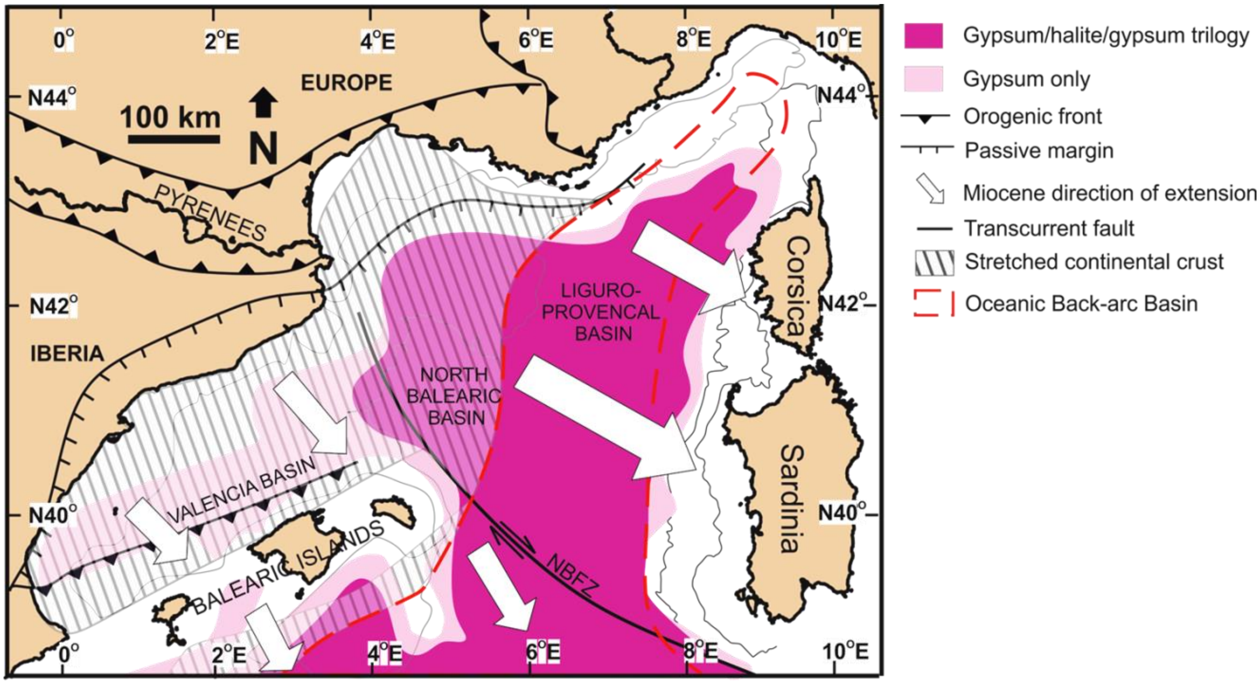

Figure 2: Tectonic and salt distribution map of the West Mediterranean passive margin system, Miocene rifting and subsequent formation of the North Balearic and Liguro-Provençal Basins from slab roll back of the Corsica (Co), Sardinia (Sa) and Calabria (Ca) (Gunnell et al 2008), (Maillard et al 2003), (Droz et al. 2006).

Study aims

We apply minibasin scale halo-kinematic sequence-stratigraphic concepts from (Mianaekere and Adam 2020) for the detailed analysis of syn-kinematic depositional sequences to further investigate local controls of diapir growth and creation of accommodation space in related salt-withdrawal minibasins. This study combines the concepts of halo-kinematic sequence stratigraphy based on the identification of unique internal depositional patterns within minibasin sequences [see also (Aschoff and Giles 2005; Hudec et al. 2009; Madof et al. 2009; Mannie et al. 2014)] with the concepts of pre-kinematic and syn-kinematic basal megaflaps

(Nikolinakou et al. 2017; Rowan et al. 2016) and halokinetic sequences (Giles and Lawton 2002; Kernen et al. 2012; Rowan et al. 2003) which employ recognition of structural geometries of depositional packages associated with diapir growth (Fig. 3), further discussed in section 2.

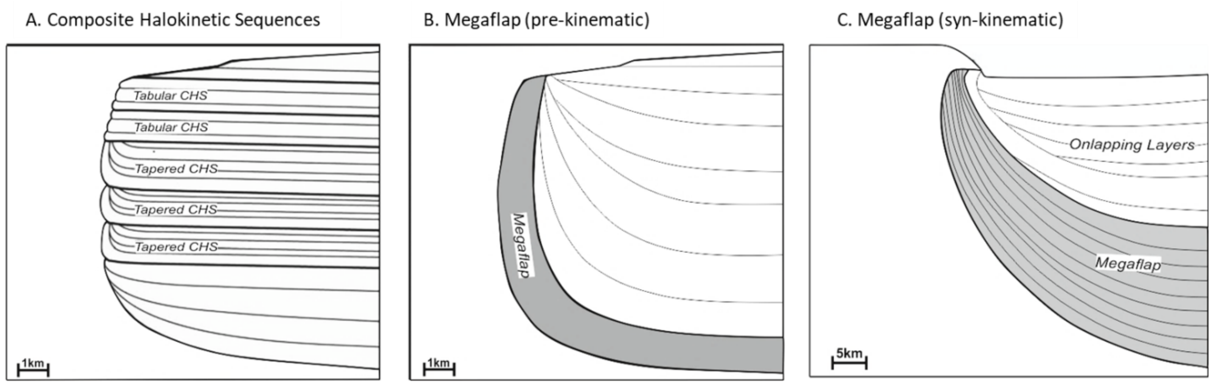

Figure 3: Published structural geometries of genetic halokinetic sequence packages critical for understanding diapir evolution. A. Stacked Composite Halokinetic Sequences defined by differences in shape and geometry of drape folds adjacent to passive diapirs (Giles & Rowan 2012, Rowan et al. 2016). B. Megaflap (Pre-kinematic), defined by several kilometer fold widths and structural relief (Rowan et al. 2016). C. Megaflap (syn-kinematic), defined by upturn of thick formerly roof sediments with onlap of younger downbuilding sediments (Nikolinakou et al. 2017).

Identification of unique internal stratal patterns within minibasin sequences and structural geometries of related depositional packages typical of each syn-kinematic growth phase or stage (Jackson and Hudec 2011) of salt structures may enable a better understanding of local halokinetic processes and intermittent response to regional contraction (Duffy et al. 2017).

Understanding of regional contractional salt tectonics and the evolution of a diapiric and minibasin domain has so far been driven by detailed seismic studies (Adam et al. 2012; Brun and Fort 2011a; Brun and Fort 2004; Gottschalk et al. 2004; Tari et al. 2003; Vendeville et al. 1990) and scaled analogue experiments e.g. (Adam et al. 2005; Adam et al. 2006; Adam and Salt

Dynamics Group 2008; Gemmer et al. 2004; Ings et al. 2004; Schreurs et al. 2003). On the other hand, local-scale salt halokinesis and resulting conforming stratal architectures and stratal depositional patterns within genetic stratigraphic packages are interpreted proximal to diapirs mostly on outcrops (Andrie et al. 2012; Giles et al. 2004; Giles and Rowan 2012; Ribes et al. 2015; Saura et al. 2016). This study utilizes 2-Dimensional seismic data and is focused on the depositional packages within contractional minibasins in the west Mediterranean basin, with implications for other passive margins with salt tectonics. Further aims of this study are to:

1. Identify small-scale minibasin depositional and structural geometries evident of minibasin response to regional contraction
2. Identify local influences of diapir growth, salt-withdrawal style and sequence depositional style on temporal structural configurations and depositional patterns respectively within minibasins.
3. Analyse and demonstrate intermittent local halokinetic events on minibasin scale using halokinetic wheeler and structural wheeler diagrams.
4. Identify characteristic salt kinematic sequences for different stages of diapir growth and minibasin down-building using schematic structural restorations.

2. Comparative studies

Halo-kinematic sequence stratigraphy, Halokinetic sequence stratigraphy and megaflap

In this section, we highlight and compare established concepts of structural geometries and depositional sequences within salt-related minibasins. A comparative distinction between minibasin halo-kinematic sequence stratigraphic classifications defined by stratal depositional patterns (Mianaekere and Adam 2020) with published classifications of composite halokinetic sequences (Giles and Rowan 2012), drag fold (Schultz-Ela 2003; Schultz-Ela et al. 1993) and megaflap (Maria A. Nikolinakou and Flemings 2017; Rowan et al. 2016) defined by stratal structural geometries is shown in (Fig. 4).

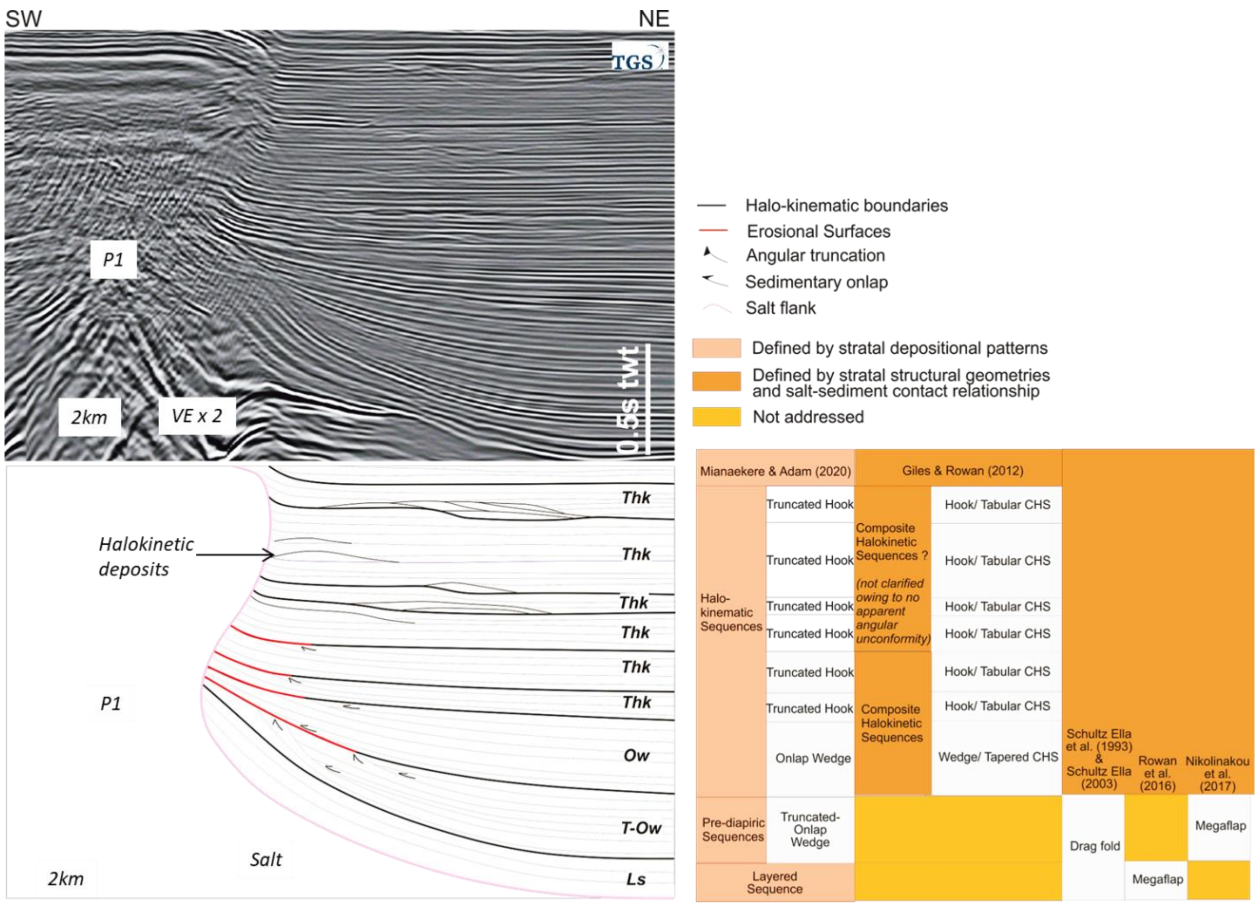

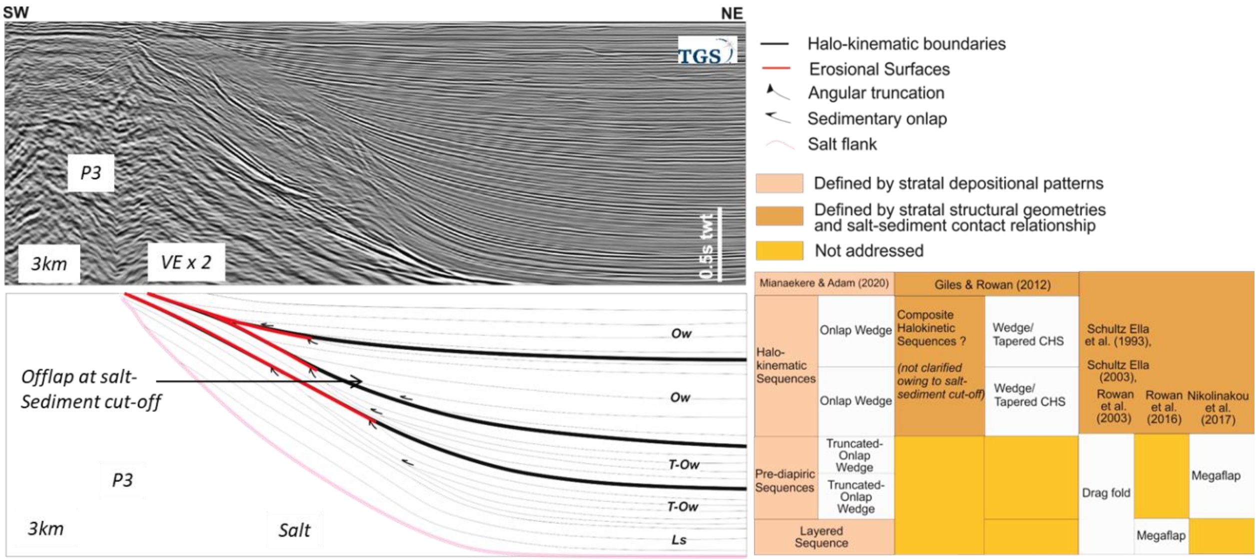

Figure 4: Comparison table showing classifications of minibasin depositional packages established for deepwater contractional diapir-minibasin profiles P1 and P3 in precedent study (Mianaekere and Adam 2020) defined by stratal depositional patterns to published classification defined by stratal structural geometries. See table 1 for clarification of terminologies and abbreviations.

In the deepwater Liguro-Provençal basin, the P1 diapir located in the distal contraction domain features a shortened (necked) salt stock. The P3 diapir located in the proximal contraction domain features an un-shortened, flared base diapir (see section 4). The pre-kinematic layer and pre-diapiric sequence are common to both P1 and P3 profiles. However the succession and salt-sediment relationship of halo-kinematic sequences for P1 and P3 profiles are different. The minibasin sequence successions between the P1 and P3 profiles are further explained in section 4 from dip and strike profile regional contraction trend and evolution.

Also, the minibasin stratigraphic classifications developed in Mianaekere and Adam (2020) and in this study builds on previously published classification schemes of active and passive kinematic phases of salt growth and pre-kinematic and syn-kinematic stages of minibasin evolution/downbuilding [see Hudec et al. (2009), Alsop et al. (2016)] shown in (Table 1).

Minibasin sequence classification based on stratal depositional or fill patterns *(Mianaekere & Adam 2020)*	Minibasin sequence classification based on stratigraphic structural configuration	Minibasin sequence evolution phase	Salt kinematic growth phase
• **Layered**: Parallel beds, homogenous to semi-homogenous thickness beds • Pre-kinematic Layer (pkl) or Layered sequence (Ls)	**Pre-kinematic megaflap**: Basal folded strata with parallel beds, defined by several kilometre fold widths and structural relief *(Rowan et al. 2016)*	Pre-kinematic	Early stage active growth
• **Truncated Onlap Wedge (T-Ow):** drape folded strata on-lapped by ponded sediments • Pre-diapiric sequence (pds)	**Syn-kinematic megaflap**: Basal folded strata, defined by upturn of thick formerly roof sediments with onlap of younger downbuilding sediments *(Nikolinakou et al. 2017)*	Early syn-kinematic	Late stage active growth
• **Onlap wedge (Ow):** Ponded sediments onlap on lower sequence boundary, convergent strata, angular truncations on upper sequence boundary • Halo-kinematic sequence (Hks)	**Wedge halokinetic sequence/ Tapered composite halokinetic sequence:** Folded convergent boundaries and broad zones of upper boundary erosion in the near-diapir zone *(Giles & Rowan 2012)*	Late syn-kinematic	Passive growth
• **Truncated hook (Thk):** No ponded sediments in sequence layer, angular truncations on upper sequence boundary or an accumulation of slump (halokinetic) deposits. • Halo-kinematic sequence (Hks)	**Hook halokinetic sequence/ Tabular composite halokinetic sequence:** Folded angular boundaries and narrow zones of upper boundary deformation in near- diapir zone halokinetic sequence *(Giles & Rowan 2012)*	Late syn-kinematic	Passive growth

Table 1: Clarification of terminology

Halo-kinematic sequence stratigraphy was established in (Mianaekere and Adam 2020) on near-diapir scale and is developed in this study on minibasin scale to analyse the creation of accommodation space in related salt-withdrawal minibasins and the spatial-temporal changes in depositional patterns respectively within minibasins. A comparative analysis of formation of halo-kinematic sequences on minibasin scale is demonstrated with diagrammatic cross-sections from studies of the Emirhan minibasin in the Sivas Basin, Turkey (Ribes et al. 2015). Cross sections of the Emirhan minibasin shows subsidence through time and geometric successions of hook and wedge halokinetic sequences (Fig. 5). Figure 5 demonstrates 1) how the relationship between net diapir rise rate and net local sediment accumulation rate has led to the bathymetric failure or erosion of material at the diapir crest creating a hook or wedge halokinetic sequence 2) how the differential growth rates between bounding diapirs influence the creation of accommodation space within successive local depocentres i.e. a shift in depocentre from minibasin center to a rim focused localized depocentre. (Andrie et al. 2012; Giles et al. 2004; Giles and Rowan 2012; Kernen et al. 2012; Rowan et al. 2012a; Rowan et al. 2003)

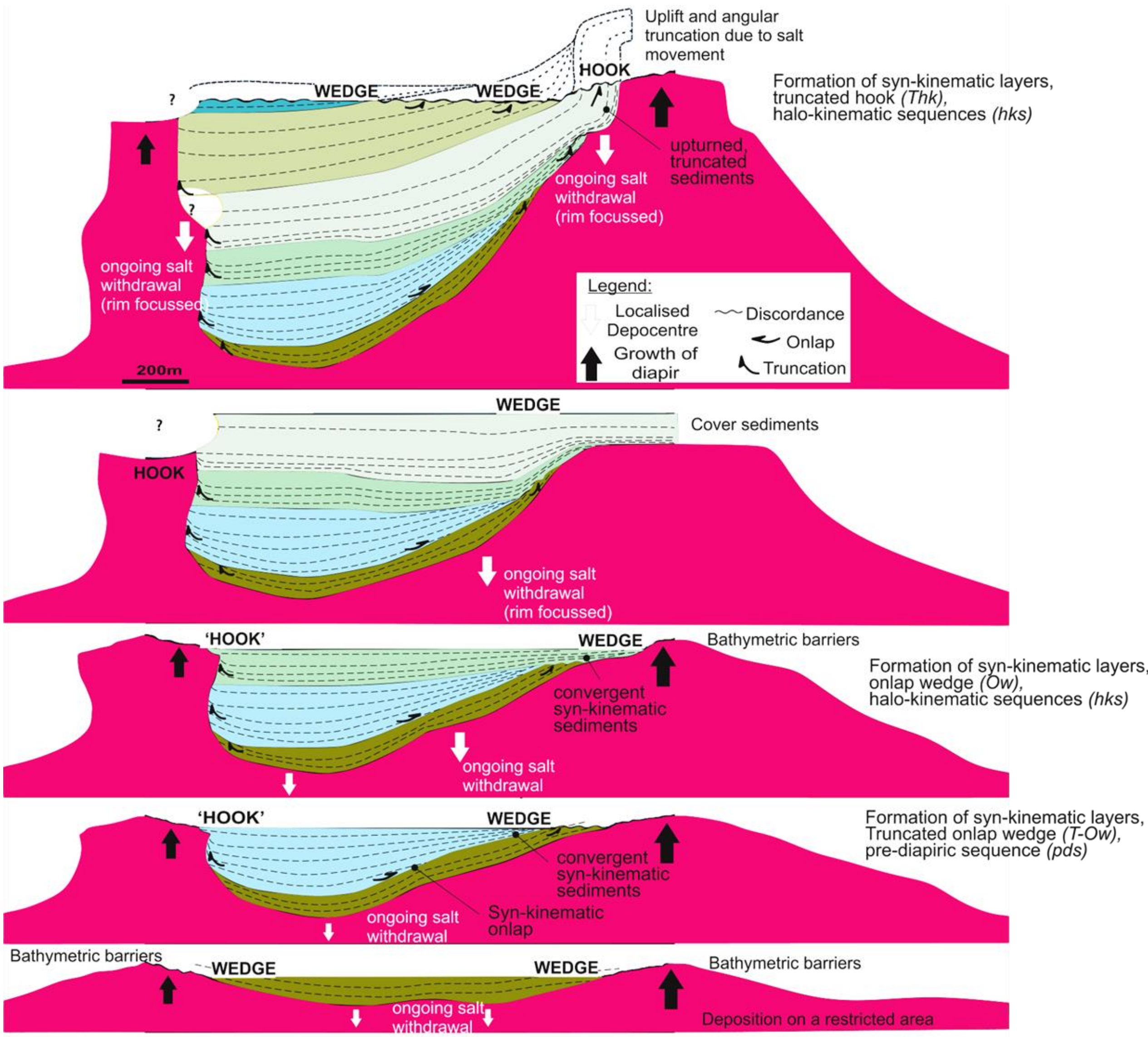

Figure 5: Diagrammatic cross-sections of the Emirhan minibasin in the Sivas Basin, Turkey illustrating subsidence through time showing formation of hook and wedge halokinetic sequences (Modified from Ribes et al. 2015). This classification can be compared to the formation of truncated onlap wedge pre-diapiric sequences and onlap wedge, truncated hook style halo-kinematic sequences. See Table 1 for clarification of terminology and abbreviations.

3. Methodology

Seismic stratigraphic interpretation

A high-resolution seismic-stratigraphic analysis delineated by four major high amplitude post-salt horizons (pslt-1 to pslt-4) (Fig. 6) have been correlated across a wide coverage 2-dimensional seismic survey spanning from continental shelf to distal deep basin and across minibasins in the Liguro-Provençal basin [see Mianaekere and Adam (2020)]. The four post-salt horizons can be correlated with the regional tectono-stratigraphic and regional sequence stratigraphic framework of the Liguro-Provençal basin (Roberts and christoffersen 2013) and thereby further constrain a detailed local minibasin scale halo-kinematic sequence-stratigraphy analysis for the deepwater contractional diapiric province.

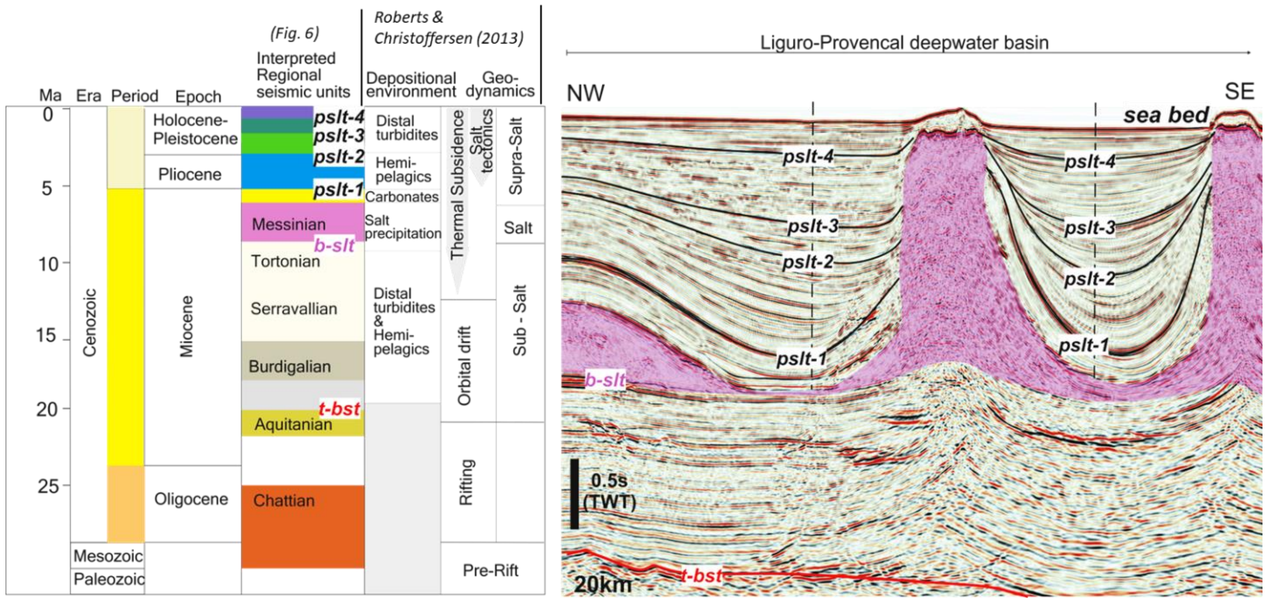

Figure 6: Minibasin seismic stratigraphy in the deepwater Provençal basin (right) and stratigraphic chart with regional sequence-stratigraphic units of the Liguro-Provençal Basin (left).

Geodynamics of post Messinian stratigraphy includes continued thermal subsidence of the distal deepwater basin relative to the continental shelf margin influencing regional salt tectonics in the supra-salt (Roberts and christoffersen 2013) between pslt-1 to pslt-4 (Fig. 6). Regional depositional sequence stratigraphic interpretation derived from trajectory interpretation of delta/shoreline and shelf margin clinoforms in continental shelf and seismic facies analysis of the proximal slope and basin plain was sourced from Mianaekere and Adam (2020). In figure 6, sequence stratigraphic units between the reflection free Messinian halite unit and carbonate unit bound by pslt-1 relate to the Mediterranean base level drop during the Messinian (Bache et al. 2015; Bache et al. 2009; Rouchy and Caruso 2006). Pliocene depositional sequence unit between pslt-1 and pslt-2 are observed to be widely deposited on the paleo slope and paleo basin plain controlled by a major sea level rise. Hemipelagic sedimentation is interpreted between pslt-1 and pslt-2 in the deepwater basin. Sequence units between pslt-2 to pslt-4 consist largely of chaotic, turbiditic facies in the distal basin plain related to the late Pliocene to Pleistocene Rhone fan turbidite system in deepwater (Mianaekere and Adam 2020; Roberts and christoffersen 2013).

Halokinetic wheeler diagrams

Syn-kinematic minibasin sequence packages are delineated from the depositional patterns. The local temporal halokinetic processes, e.g. nature of erosion and sediment infilling can be visualised by wheeler diagrams (Mianaekere and Adam 2020). The wheeler diagram is a 2D representation of the interpreted geo-seismic section with relative geological time as the vertical axis and section position in meters as the horizontal axis (Wheeler 1958). Each geological stratum in the cross section is plotted at a relative geological time line and extrapolated horizontally according to its measured line length in the interpreted geo-seismic section. Stratal thicknesses on the wheeler diagrams are diagrammatic representations obtained from the time-migrated geo-sections. The derived stratal thicknesses and inclinations of surfaces demonstrate relative timescales or rates of deposition to rates of associated salt rise.

Schematic structural restoration of diapir-minibasin profiles

For the analysis of the depositional and structural cycles and overall evolution of the minibasins, Interpreted diapir-minibasin sections are sequentially restored by flattening of key seismic-stratigraphic horizons. It is important to note that this seismic horizon flattening produces only a schematic restoration and does not consider decompaction of the sediments or isostatic adjustment of the base-of-salt usually being performed for the construction of a structurally balanced section restoration (Hudec 2003; Rowan and Ratliff 2012). The flattening process preserves bed lengths in adjacent minibasins. Cross-section restoration typically assumes plane-strain deformation and area conservation, constraints that are usually invalid for the salt layer itself because of its characteristic three-dimensional flow and possible dissolution, and for supra-salt layers because of the variable movement directions of separate minibasins or vertical-axis rotation during translation above salt (Rowan and Ratliff 2012). Orientation of the cross-section is therefore chosen parallel to the tectonic transport direction of the overburden strata in downslope direction due to the gravitational processes (Rowan and Ratliff 2012). In summary, the kinematic restorations may not account for thinning of sedimentary layers caused by shear strain due to active diapir piercement (Hudec and Jackson 2007), out-of-section deformation, and diapiric shapes resulting from lateral deformation and mechanical drag folds (Nikolinakou et al. 2017).

Structurally restored wheeler diagram

The sequentially restored cross-sections have been complemented by a series of restored structural wheeler diagrams. The structural deformation derived from each restoration stage is overlain in the structural wheeler diagram with separate colour overlays according to the line length of the given geological strata affected by structural deformation. The colour overlay delimits the extent of structural deformation for each geological stratum onto the wheeler diagram.

4. Contractional salt kinematics

Contractional salt tectonics in the Provençal deepwater basin is governed by thin-skinned salt-detached gravity-driven deformation. The Contractional domain is separated from the landward extensional domain by an intermediate transitional domain underlying the continental slope (Bonnel et al. 2005; dos Reis et al. 2005; Granado et al. 2016; Leroux et al. 2015; Maillard et al. 2003; Mianaekere and Adam 2020). Contractional overprinting of former halokinetic salt structures like salt pillows and salt-cored anticlines that proof the landward migration of the contractional domain since the Late Pliocene can be observed in dip seismic profiles (Fig. 7) and (Fig. 8).

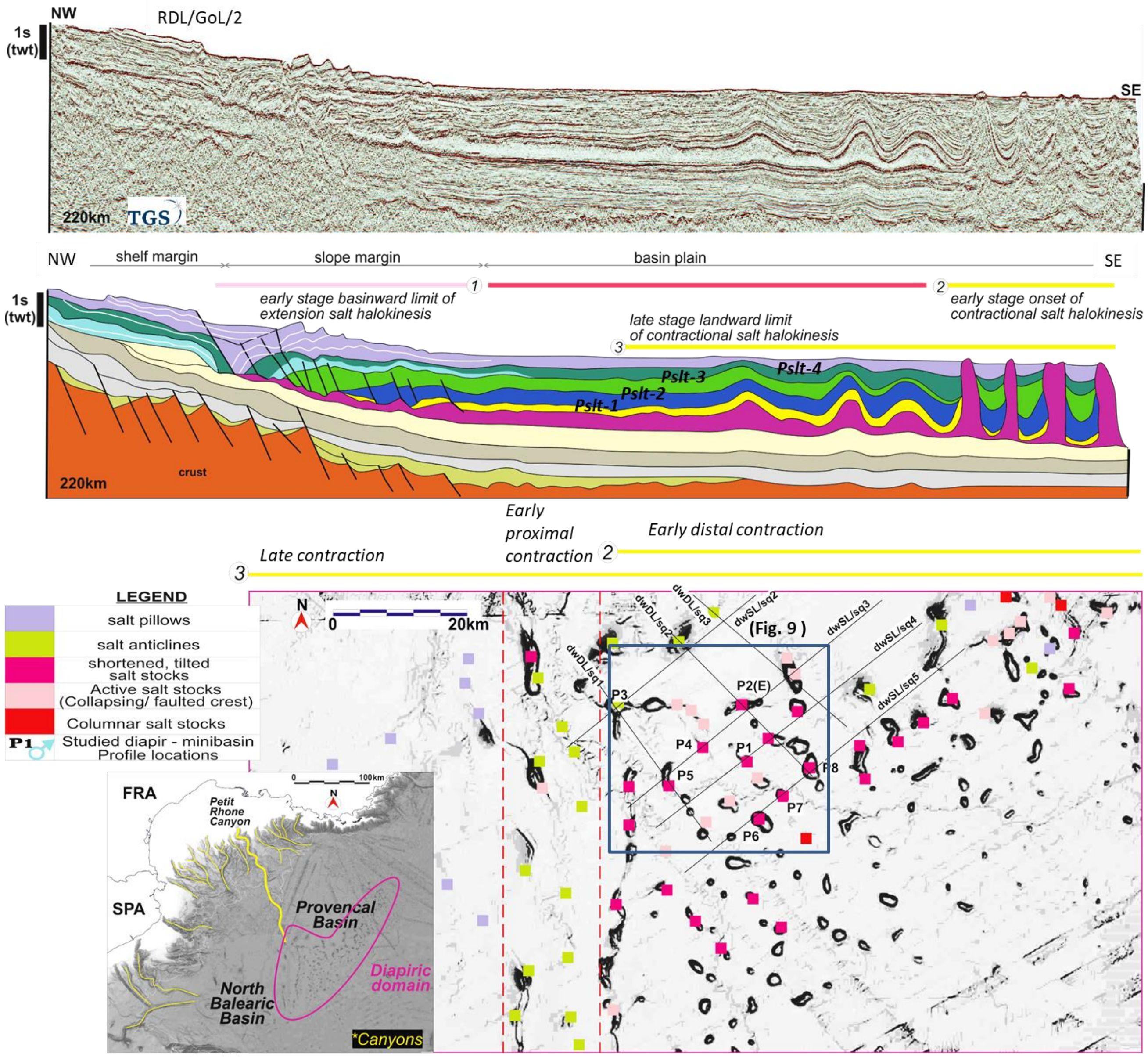

Figure 7: Bathymetric map of the Western Mediterranean reproduced from the GEBCO (*www.gebco.net/dgridded_bathymetry_data/)* showing sediment transport pathways and the location of the diapiric domain. Within the diapiric domain the location of deep water strike line (dwSL) in sequence (sq) (dwSL/sq2 to dwSL/sq5), deepwater dip lines (dwDL) (dwDL/sq1 to dwDL/sq3) and the location of studied diapir profiles (P1) are shown.

Contractional salt tectonics in the Provençal deepwater basin is analyzed from NW-SE trending dip lines dwDL/sq1, dwDL/sq2 and dwDL/sq3 (Fig. 8) and SW-NE trending strike lines dwSL/sq2, dwSL/sq3, dwSL/sq4 and dwSL/sq5 (Fig. 9). Spatial variation of contraction styles and shortening in the early stage distal contraction domain are evident by the variation of salt structural geometries, minibasin geometries and timing of syn-kinematic subsidence in minibasins interpreted on the dip and strike seismic sections. The contractional domain represents the major sediment sink in the deepwater Provençal Basin. Hence, the subsidence history in salt-withdrawal minibasins is recorded in the variation of stratigraphic thicknesses in early (dark grey) and late (light grey) syn-kinematic depositional sequences (Fig. 8) and (Fig.9).

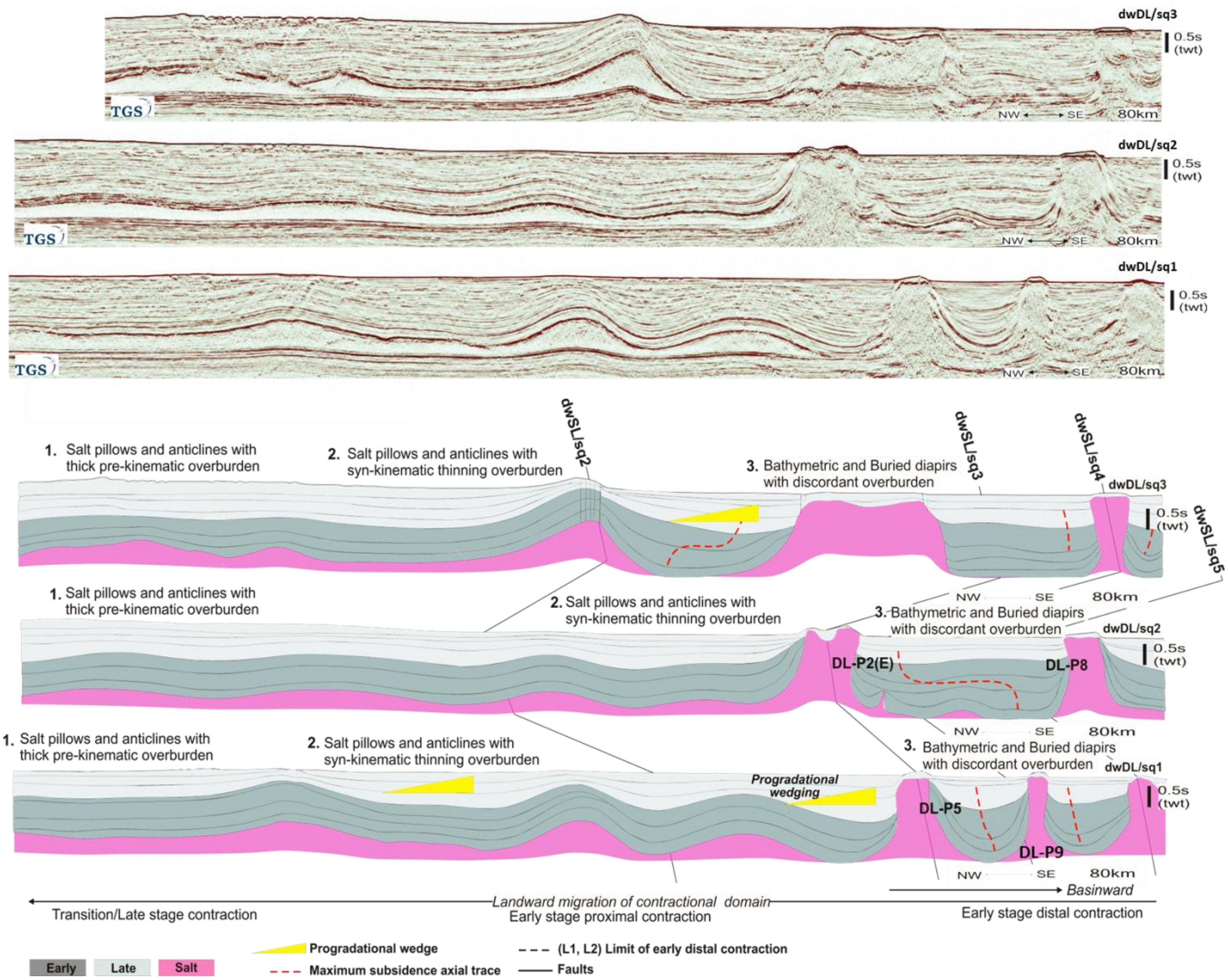

Figure 8: Un-interpreted and interpreted NW-SE trending seismic DIP sections perpendicular to the Gulf of Lion shelf margin. Observe variation of salt structural styles, minibasin geometries and variations in timing and intensity of syn-kinematic subsidence in minibasins across the sections. Note shortening labels 1 to 3 used to indicate intensity of shortening, minimum shortening 1 to maximum shortening 3.

The NW-SE trending dip lines (Fig. 8) show a progressive segmentation in basinward direction in contractional sub-domains consisting of an early transitional/late stage contractional, early stage proximal contractional and early stage distal contractional sub-domain. The intensity of shortening of salt structures in each sub-domain is indicated by labels 1 (minimum) to 3 (maximum). In the landward early transitional/late stage contractional zone, minor shortening (1 in Fig. 8) is represented by low-medium amplitude salt pillows and salt-cored anticlines with thick pre-kinematic overburden. In the early stage proximal contractional domain, moderate shortening (2 in Fig. 8) is represented by salt pillows and salt-cored anticlines with syn-kinematic thinning in overburden. In the early stage distal contractional domain, maximum shortening (3 in Fig. 8) is represented by tall diapirs with bathymetric expressions and discordant overburden.

The early sage distal contraction is further analysed from SW-NE strike sections in the deepwater contractional province (Fig. 9). The boundary of the early distal contraction (L1 in Fig. 9) is indicated in the SW part of the strike seismic profiles. The boundary is indicated by compressional salt pillows terminating at bathymetric diapirs and active salt diapirs. In the NE part of the strike seismic section the boundary of the early distal contractional domain (L2 in Fig. 8) is marked by contractional diapirs and active contractional salt anticlines.

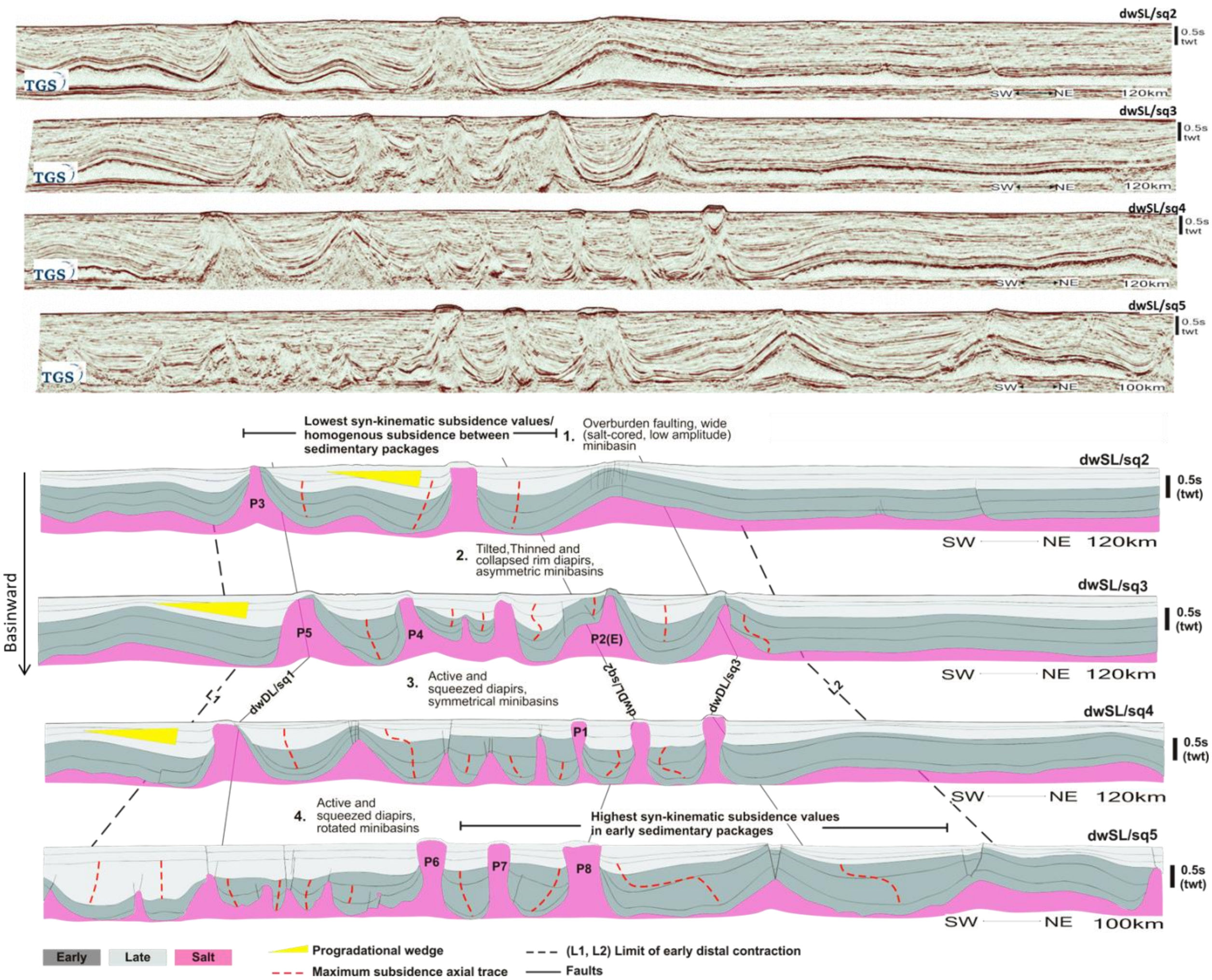

Figure 9: Un-interpreted (top) and interpreted (bottom) SW-NE trending 2-Dimensional seismic STRIKE lines parallel to the Gulf of Lion shelf margin. Observe variation of salt structural styles, minibasin geometries and variations in timing and intensity of syn-kinematic subsidence in minibasins across the sections. Note shortening labels 1 to 4 used to indicate intensity of shortening, minimum shortening 1 to maximum shortening 4.

The SW limit of early distal contraction L1 coincides with the basinward termination of the progradational sedimentary wedge against the furthest landward contractional diapir (see Mianaekere and Adam 2020). The NE limit of early distal contraction L2 also indicates the maximum basinward extent of contractional diapirs and contractional minibasins. Landward migration of the contraction domain is also recorded the subsidence history in salt-withdrawal minibasins across the strike seismic profiles (Fig. 9) showing the variation of stratigraphic thicknesses in early and late syn-kinematic depositional sequences. Maximum syn-kinematic ‘subsidence values’ are recorded in early sedimentary packages within minibasins furthest in the contractional province on seismic profile dwSL/sq5 (Fig. 9) while minimum syn-kinematic ‘subsidence values’ are recorded in early sedimentary packages within minibasins most proximal in the contractional province on dwSL/sq2 (Fig. 9).

Relative intensity of shortening across the strike seismic profiles vary from 4-maximum on dwSL/sq5 to 1-minimum on dwSL/sq2 (Fig. 9). DwSL/sq5 being the furthest from margin, exhibits salt structures and minibasins with greater intensity of shortening. Maximum shortening (4) on dwSL/sq5 shows active diapirs to the SW and significantly squeezed (necked) diapirs to the NE bound rotated minibasins between P6, P7 and P8 diapirs (discussed in section 5). Shortening (3) on dwSL/sq4 shows active diapirs bound symmetrical minibasins and significantly squeezed (necked) diapirs bound asymmetric minibasins. Shortening (2) on dwSL/sq3 shows tilted, thinned and collapsed rim diapirs with flared base bound asymmetric minibasins. Minimum shortening observed on dwSL/sq2 shows faulting of concordant overburden above salt pillow and wide salt cored minibasins with widths of ca. 20km adjacent to P3 diapir in comparison to ca. 10km minibasin widths on dwSL/sq3, between P5 and P4 and north east of P2 (E), ca. 5km minibasin widths on dwSL/sq4 NE of P1 and ca. 4km to 5km on dwSL/sq5 between P6 and P7 and P8. Another crucial observation from strike seismic profiles (Fig. 8) is variation in length of flexural upturn of basal sedimentary layers against salt diapirs (further discussed in 7). The more proximal, landward strike profiles host large length upturns observed adjacent to P3, P5, P4 and P2 (E) diapirs and basinward, furthest strike profile host shorter length scale upturn adjacent to P1, P6, P7 and P8 diapirs.

5. Minibasin Sequence Stratigraphic analysis

An interpolated isochron map of post-salt sediments derived from 2D whole seismic survey shows concentration of thickest post salt sediments and minibasin fill in the distal deepwater, contraction province (Fig. 10). The contour overlay (Fig. 10) is computed with a flex grid interpolation algorithm. Extracted trends from flex grid contour overlay show interpreted salt stocks (black circles), trends and connectivity of salt peaks/salt walls (white lines) in the contractional province corroborated with bathymetric map (Fig. 7, section 4). Area of blind minibasins (Fig. 10) i.e. partially surrounded by salt walls and stocks (Banham and Mountney 2013) range from 54sqkm (MB-2, Fig. 10) to smaller minibasins 20sqkm (MB-4, Fig. 10) further basinward in the early distal contraction domain.

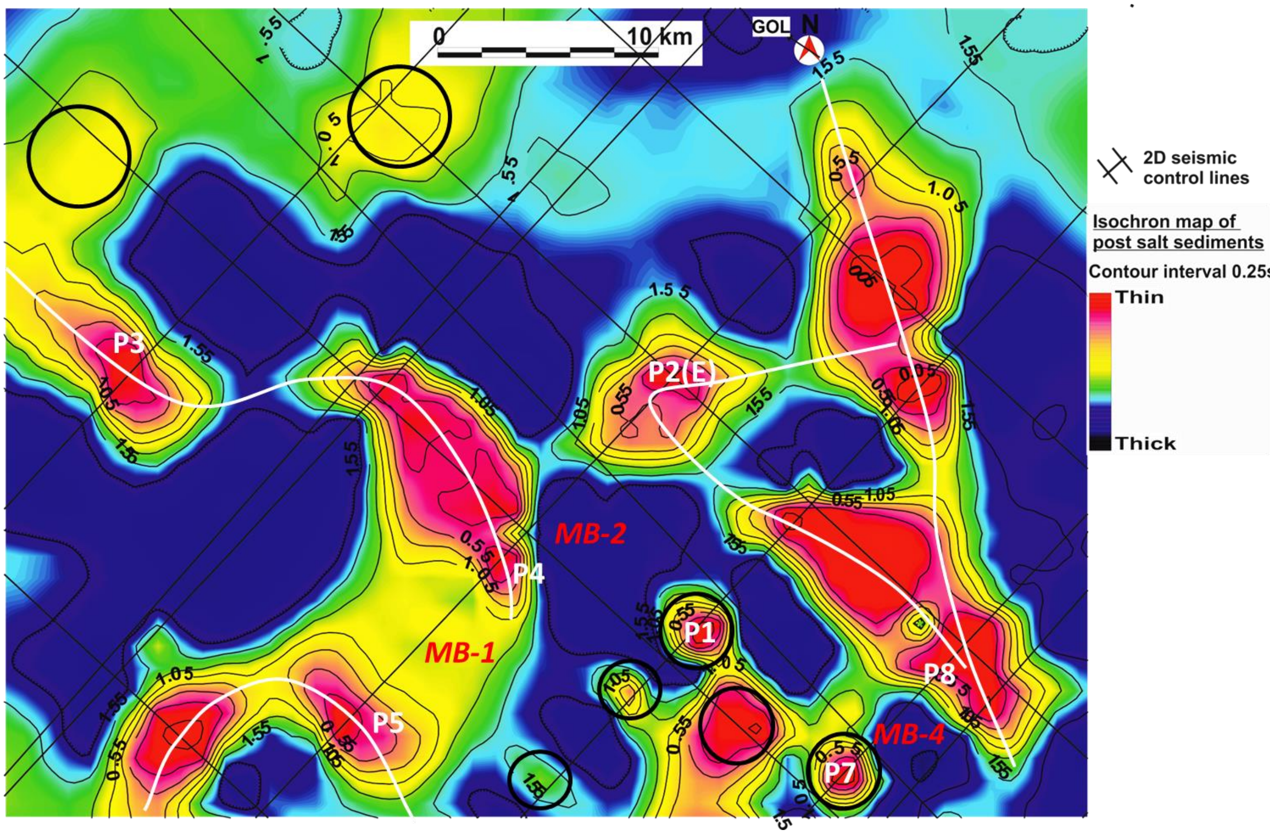

Figure 10: Isochron map of post-salt sediments showing locations of some minibasin profiles investigated in this section. Map location shown on Fig. 7. Suggested salt stocks (black circles) and salt walls (white lines) backed by bathymetric map shown in Fig. 7.

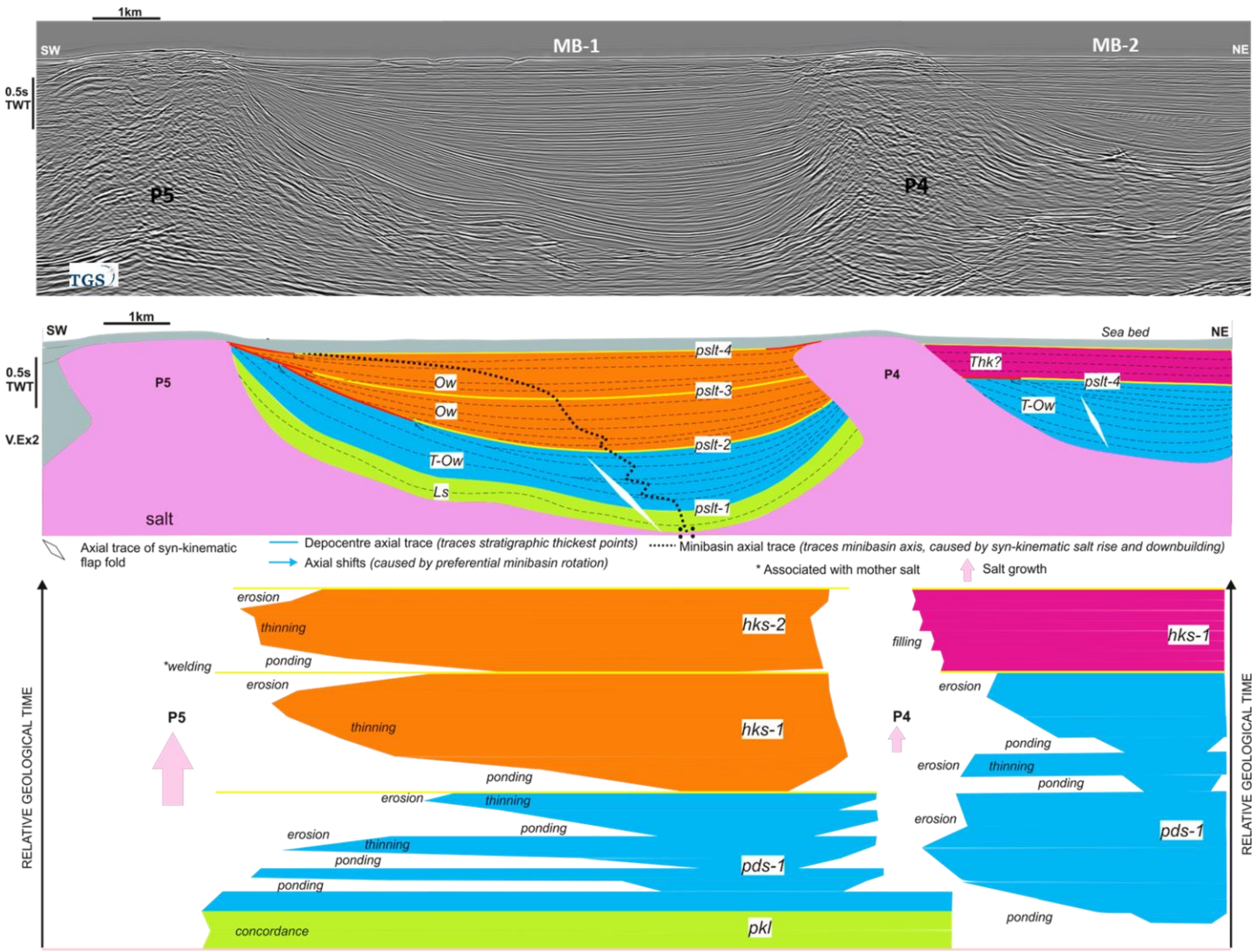

Figure 11: Un-interpreted (top) and interpreted seismic sections (middle) and halokinetic wheeler diagram (bottom) of the P4 and P5 strike diapir-minibasin profile. [Light green - pre-kinematic layer/layered sequence, light blue – pre-diapiric/truncated onlap wedge sequence, orange – halo-kinematic/onlap wedge sequence, purple – halo-kinematic/truncated hook sequence] refer to section 3, table 1.

The diapirs P4 & P5 (Fig. 11) are tilted in SW direction of regional tectonic transport, hence a minibasin symmetry skewed preferential to the SW tilt. Angular halo-kinematic boundaries on the NE flank of diapir P5 and a depocenter axial trace skewed to the P5 diapir suggest a significant variation in growth rates between the bounding diapirs P5/P4 through time. Seismic stratal patterns within the minibasin depositional sequences consist of one layered sequence (Ls), one truncated onlap wedge sequence (T-Ow) and two onlap wedge sequences (Ow). Hence, in the wheeler diagram of the minibasin between P4/P5, distinct kinematic sequences consist of one pre-kinematic layer (pkl), one syn-kinematic pre-diapiric sequence (pds) and two halo-kinematic sequences (hks).

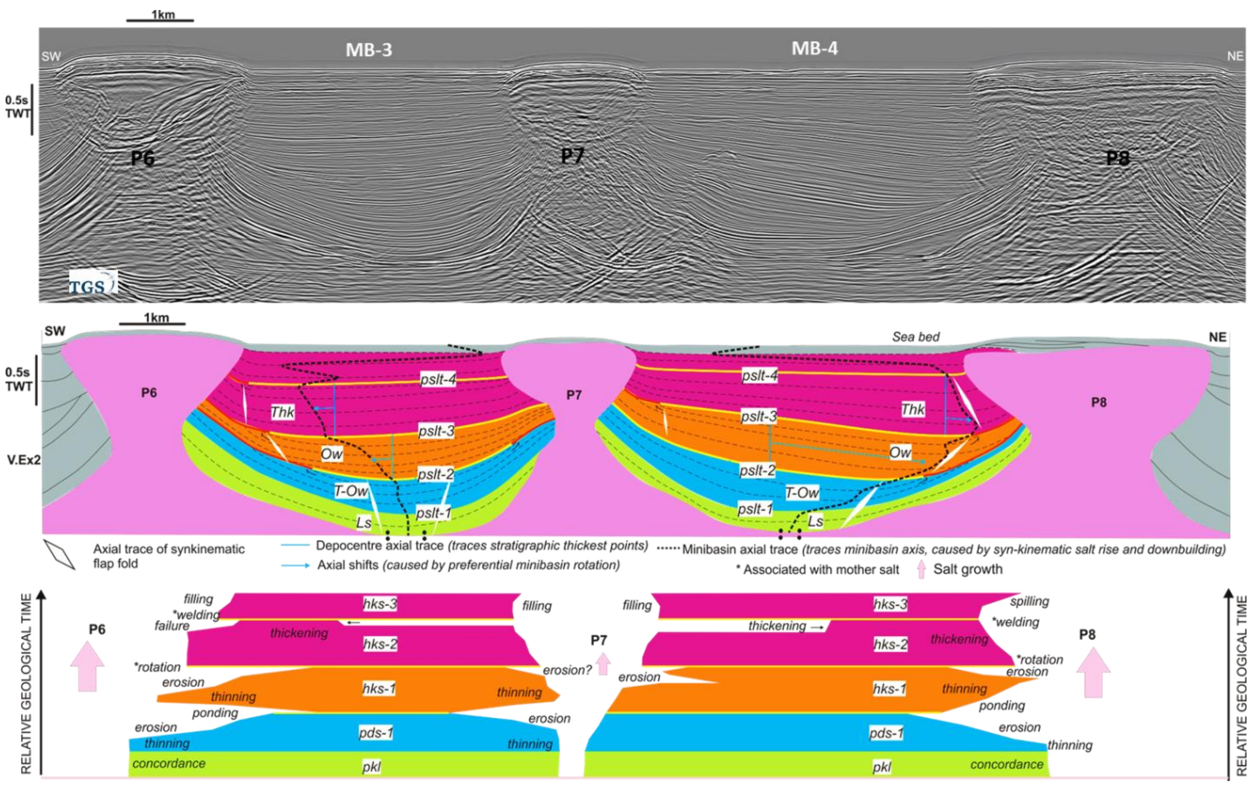

Figure 12: Un-interpreted (top) and interpreted seismic interpretation (middle) and halokinetic wheeler diagram (bottom) of the P6, P7 and P8 strike diapir-minibasin profile. [Light green - pre-kinematic layer/layered sequence, light blue – pre-diapiric/truncated onlap wedge sequence, orange – halo-kinematic/onlap wedge sequence, purple – halo-kinematic/truncated hook sequence] refer to section 3, table 1.

The diapirs P6, P7 & P8 (Fig. 12) are vertical and mostly symmetrical salt stocks with a characteristic hourglass geometry with a neck and bulbous head indicating late-stage, ongoing contraction. The minibasin profile between diapirs P6/P7 shows angular halo-kinematic boundaries on both flanks of the minibasins in the pre-diapiric sequence, suggesting no significant variation in growth rates of bounding diapirs at the time. Subsequent halo-kinematic sequences show angular halo-kinematic boundaries on the minibasin flank to the more rapidly growing diapir P6 as indicated by a depocenter axial trace advancing towards diapir P6 in younger minibasin depositional sequences. In the P7/P8 minibasin profile, P8 diapir is the faster growing diapir through time and is evident from erosional halo-kinematic terminations in each stratigraphic sequence and a minibasin axial trace skewed towards diapir P8. Diapir P7 has no apparent erosional terminations on either side of the truncated hook sequences (Thk) which may suggest the absence of bathymetric relief due to ceasing salt flow into the diapir. Seismic stratal patterns within sequence packages in minibasin between diapirs P6 & P7 (Fig. 12), P7 & P8 (Fig. 12) consist of one layered sequence (Ls), one truncated onlap wedge sequence (T-Ow), one onlap wedge sequences (Ow) and two truncated hook (Thk) sequences. Hence, wheeler diagrams of minibasins between diapirs P6/P7 and diapirs P7/P8 show one pre-kinematic layer (pkl), one syn-kinematic pre-diapiric sequence (pds) and three halo-kinematic sequences (hks).

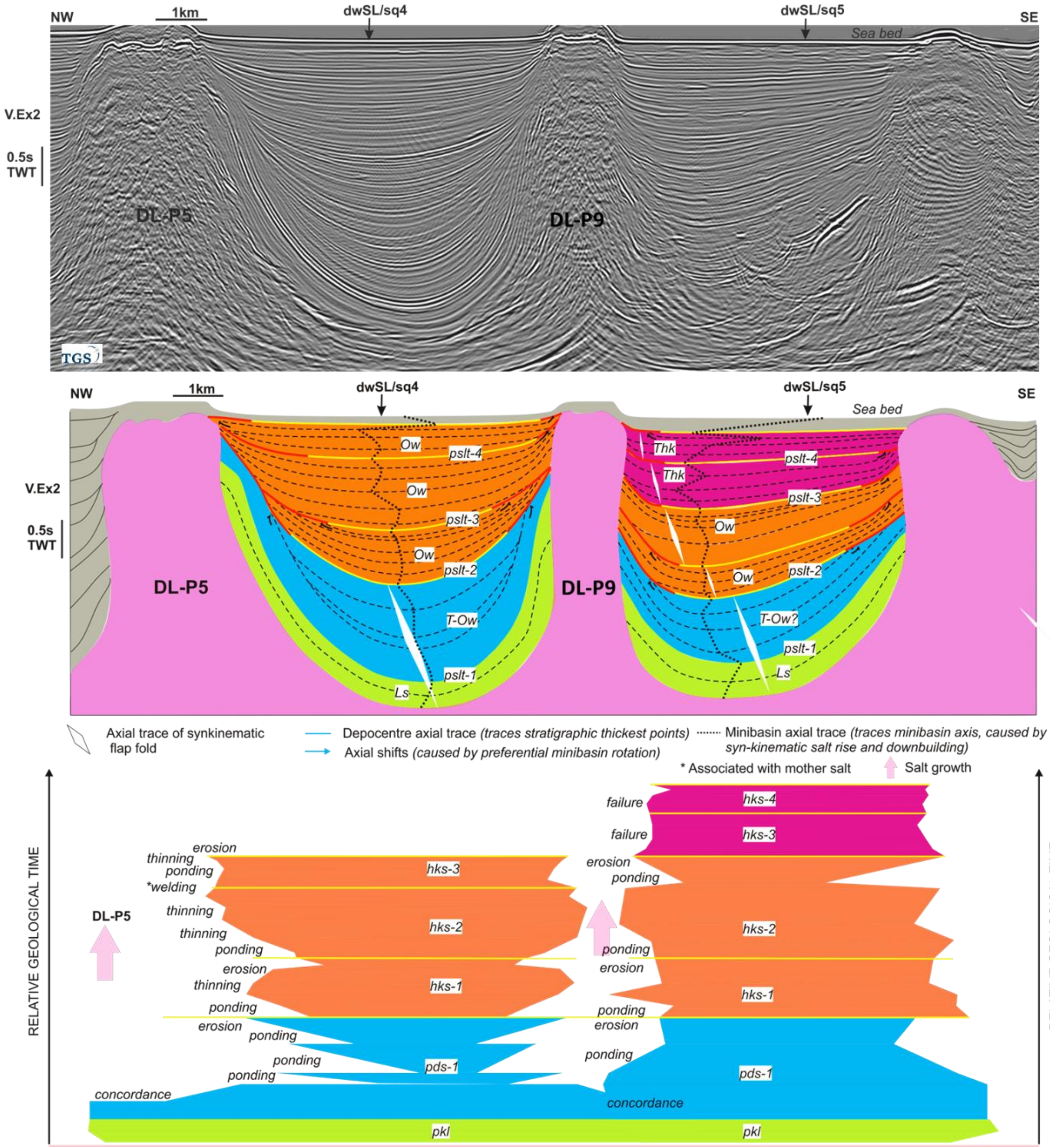

Figure 13: Un-interpreted (top) and interpreted seismic interpretation (middle) and sedimentary wheeler diagram (bottom) of the DL-P5 and DL-P9 dip direction diapir-minibasin profiles. [Light green - pre-kinematic layer/layered sequence, light blue – pre-diapiric/truncated onlap wedge sequence,

orange – halo-kinematic/onlap wedge sequence, purple – halo-kinematic/truncated hook sequence] refer to section 3, table 1.

Diapir P5 features in dip section a c. 2 km wide stem and wide base. Diapir P9 to the SE features a c. 1km wide narrow stem and a relatively narrow base. The minibasin flank adjacent to diapir P5 shows angular erosional terminations on each syn-kinematic depositional sequence i.e. the pre-diapiric and subsequent halo-kinematic sequences and a symmetric minibasin axial trace suggesting similar growth rates between bounding diapirs P5 and P9 through time. The minibasin adjacent to the diapir P9 to the SE also shows angular erosional terminations on each syn-kinematic stratigraphic sequence. However, a minibasin axial trace skewed toward the diapir P9 still suggest varying growth rates of bounding diapirs and P9 being the faster growing diapir.

The wheeler diagram show intermittent local halokinetic events in depositional successions within the minibasin stratigraphic sequences. Ponding occur during periods of high sedimentation prior to minibasin weld. Erosion/erosive processes results from topographic relief of inflating salt [see also Andrie et al (2012), Giles and Rowan (2012), Kernen et al (2012)] or in other words, bathymetric base level isostasy of folded strata above regional datum. The progressive erosive surfaces of the truncated onlap wedge and onlap wedge sequences suggest longer depositional periods and relative high ratios of sedimentation to salt rise. The truncated hook sequence with thinner stratal units and flat erosive surfaces suggest shorter depositional periods during stages of high diapir growth rates.

6. Schematic structural restorations

Schematic structural restoration is carried out for analysis of temporal structural configurations and depositional patterns respectively within minibasins. Restored temporal profiles for seismic cross section P1 (Fig. 12), P2(E) (Fig. 13) are labelled (*T.1* to *T.5)* further demonstrates formation of layered pre-kinematic sequence*,* truncated onlap wedge pre-diapiric sequence and onlap wedge or truncated hook halo-kinematic sequence developed in this study on a minibasin scale.

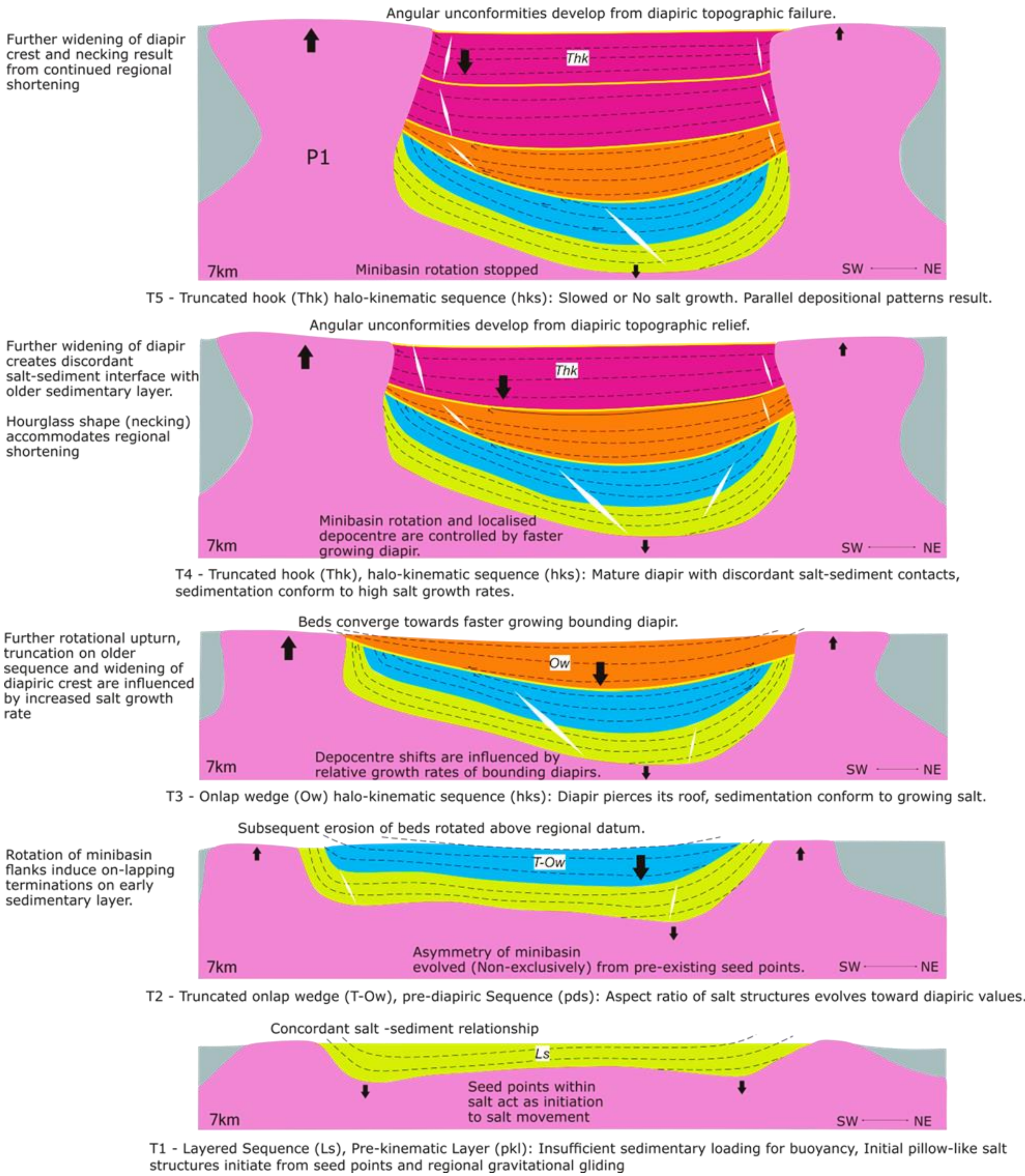

Angular unconformities develop from diapiric topographic failure.
Further widening of diapir crest and necking result from continued regional shortening
Thk
P1
7km
Minibasin rotation stopped
SW NE
T5 - Truncated hook (Thk) halo-kinematic sequence (hks): Slowed or No salt growth. Parallel depositional patterns result.
Angular unconformities develop from diapiric topographic relief.
Further widening of diapir creates discordant salt-sediment interface with older sedimentary layer.
Hourglass shape (necking) accommodates regional shortening
Thk
Minibasin rotation and localised depocentre are controlled by faster growing diapir.
7km
SW NE
T4 - Truncated hook (Thk), halo-kinematic sequence (hks): Mature diapir with discordant salt-sediment contacts, sedimentation conform to high salt growth rates.
Beds converge towards faster growing bounding diapir.
Further rotational upturn, truncation on older sequence and widening of diapiric crest are influenced by increased salt growth rate
Ow
Depocentre shifts are influenced by relative growth rates of bounding diapirs.
7km
SW NE
T3 - Onlap wedge (Ow) halo-kinematic sequence (hks): Diapir pierces its roof, sedimentation conform to growing salt.
Subsequent erosion of beds rotated above regional datum.
Rotation of minibasin flanks induce on-lapping terminations on early sedimentary layer.
T-Ow
Asymmetry of minibasin evolved (Non-exclusively) from pre-existing seed points.
7km
SW NE
T2 - Truncated onlap wedge (T-Ow), pre-diapiric Sequence (pds): Aspect ratio of salt structures evolves toward diapiric values.
Concordant salt -sediment relationship
Ls
Seed points within salt act as initiation to salt movement
7km
SW NE
T1 - Layered Sequence (Ls), Pre-kinematic Layer (pkl): Insufficient sedimentary loading for buoyancy, Initial pillow-like salt structures initiate from seed points and regional gravitational gliding

Figure 14: Kinematic restoration of the P1 diapir-minibasin profile. Five stratigraphic packages are restored from flattening individual stratigraphic boundaries. T.1 to T.5 is explained below. Refer to Fig. 16 for the structural evolution of the P1 diapir-minibasin profile.

P1 diapir-minibasin profile:

T.1 shows a pre-kinematic depocentre profile. No discordant salt-sediment contacts. Salt pillows and seed points as the initial pre-kinematic configuration are assumed, implying minimal differential loading prior to initiation of regional halokinesis. Concordant sedimentary cover is over stationary salt pillows. The pre-kinematic layers include small thickness variation around seed points located at the foot of early salt structures flanks. The seed points may remain in subsidence until the onset of kinesis. Further explanations for seed points can be seen in (Peel 2014).

T.2 shows a pre-diapiric depocentre profile. Early syn-kinematic package converges towards the rising salt structure prior to diapirism. No apparent discordant salt-sediment contacts. Sequential erosional surfaces that later form the truncated onlap wedge sedimentary pattern develops from erosion of syn-kinematic beds mechanically rotated above regional datum. The salt structure would most likely be in an active kinematic phase, penetrating a thin sedimentary roof.

T.3, *T.4*, shows syn-kinematic minibasin profiles. These syn-kinematic packages evolve in diapiric growth phase and are therefore labelled as halo-kinematic sequences in this study. Kinematic sequence boundaries are on-lapped by younger sediments or truncated by older underlying sediments. Halo-kinematic sequences occur in diapiric growth phase and are bound at top and base by unconformable kinematic sequence boundaries.

T.3 shows a halo-kinematic sequence wit convergence of syn-kinematic beds and onlaps at bottom stratigraphic boundary. A continuous salt growth at or close to regional datum can be inferred. Significant shift in localised depocentre can be observed

T.4 shows a halo-kinematic sequence with sub-parallel sedimentary layers all truncating on diapir flank. An increased salt expansion and growth may have created a relief above the diapir. Significant shifts in localised depocentre are focused towards faster growing diapir.

T.5 shows a kinematic sequence and Present day minibasin profile. *T.1* a layered sequence, *T.2* a truncated onlap wedge sequence, *T.3* an onlap wedge sequence, *T.4* a truncated hook sequence and *T.5* most likely a truncated hook sequence. A residual halo-kinematic sequence may retain as stratigraphic thinning above the salt structure.

The minibasins depocentres T.2 to T.5 migrate towards the salt structures flanks in the later stages of salt halokinesis.

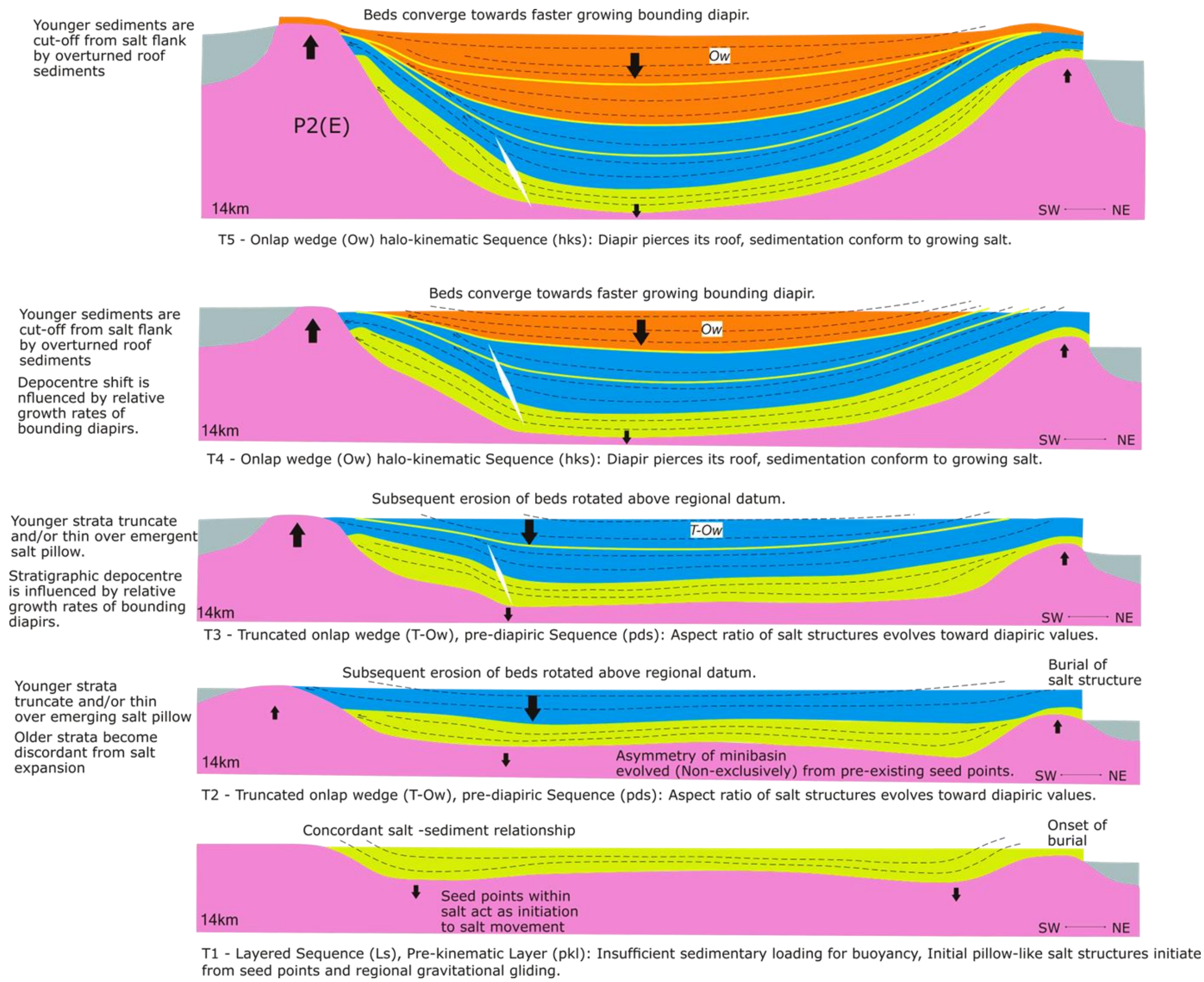

Figure 15: Kinematic restoration of the P2(E) diapir-minibasin profile. Five stratigraphic packages are restored from flattening individual stratigraphic boundaries. T.1 to T.5 is explained below.

P2 (E) diapir-minibasin profile:

T.1 shows a pre-kinematic depocentre profile. No discordant salt-sediment contacts. Concordant sedimentary cover is over stationary salt pillows. The pre-kinematic layers include small thickness variation around seed points located at the foot of early salt structures flanks. Onset of burial of adjoining salt structure is observed with implications for future growth rate and possibility for piercement.

T.2 shows a pre-diapiric depocentre profile. An early syn-kinematic package with early stage discordance and crestal thinning above an emerging salt structure is interpreted. Discordance of early pre-kinematic strata is formed from early expansion of salt pillow. Sequential erosional surfaces that later form the truncated onlap wedge sedimentary pattern develops from erosion of syn-kinematic beds plastically rotated above regional datum.

T.3 shows a pre-diapiric depocentre profile. A second syn-kinematic package converges towards an emerging salt structure. Discordance of older strata is formed from rapidly expanding salt pillow.

T.4 shows a syn-kinematic minibasin profile. A syn-kinematic package converges towards an emergent salt structure. Stratigraphic package is cut-off from salt flank by overturned minibasin flank sediments.

T.5 shows a syn-kinematic sequence and Present day minibasin profile consisting of *T.1* a layered sequence, *T.2* & *T.3* a truncated onlap wedge sequence, *T.4* & *T.5* onlap wedge sequences and *T.5,* an onlap wedge sequence with residual syn-kinematic thinning above the P2 diapir.

7. Discussion

Structural evolution of flap folding

Structural wheeler diagram of P1 diapir-minibasin profile (Fig. 16) produced from schematic structural restorations of the P1 diapir-minibasin profile (section 6), shows the evolution of drag folding [see Schultz-Ela (2003)] T1 to T5 within a downbuilding minibasin. Syn-kinematic packages generally thin and upturn towards diapir flanks. The widths of structural upturn also known as drape geometries (Schultz-Ela 2003; Schultz-Ela et al. 1993) distinguish older sedimentary packages that form megaflaps [see (Callot et al. 2016; Nikolinakou et al. 2017)] from younger syn-kinematic packages that form the halokinetic sequences [see Giles and Rowan (2012)] or halo-kinematic sequences in this study. Lithological interpretations on successive minibasin sequences (Fig. 16), extrapolated from proximal margin depositional sequence units (refer to section 3) establish influence of regional sedimentation on distal basin contractional salt tectonics. However minibasin halo-kinematic sequences in this study form in deepwater environments.

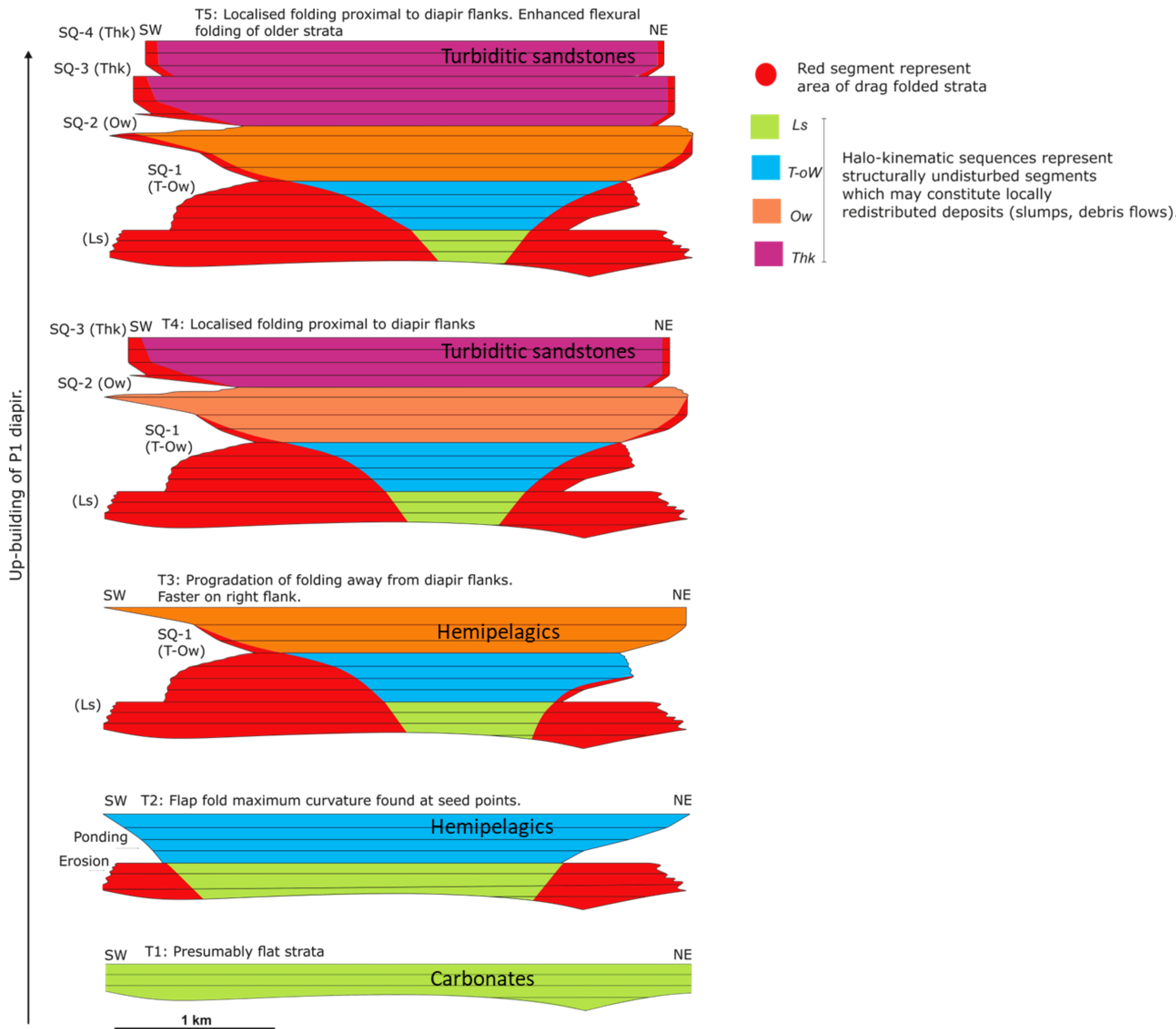

Figure 16: Structural wheeler diagram of P1 diapir-minibasin profile. Shows 1) evolution of drag folding within a downbuilding minibasin 2) drag folding styles for minibasin sequence successions

The structural wheeler diagram demonstrates 1) the transition from large length scale (100s of meters) folding to small length scale (10s of meters) folding proximal to diapir flank 2) transition from basal megaflaps to local halo-kinematic sequences. The rotation of depositional layer(s) starts with the onset of salt kinesis and downbuilding (Schultz-Ela 2003; Waltham 1997), hence the term flexural drag (Alsop et al. 2000). Preferential drag to one minibasin flank starts with differential salt growth rates of bounding diapir. Drag zones (Schultz-Ela 2003) indicated in the temporal profiles maybe categorised as 1) Large length scale folds associated with early depositional layers, these rotate from minibasin anchor points and 2) Small length scale folds associated with younger depositional layers, these rotate from local depocentre axis. The small scale length folds are associated with halo-kinematic sequences form in passive (diapiric) growth phase. The large scale length folds are associated with pre-diapiric sequences form in active (pre-diapiric) growth phase. Diapir flaring i.e. active high salt rise in the pre-diapiric growth phase and later minibasin welding enable large scale upturn/ flexural fold of the pre-diapiric sequence. Temporal profiles T.3 to T.5 shows preferential drag with faster growing diapir P1. T.5, present day configuration show minibasin weld and weld length constrain unfolded stratal segments and welded points in the mother salt that cannot be folded. Drag stops at minibasin weld time or at flanks of stationary salt.

Noteworthy, all flexural folds, small or large length scales form during active salt rise and downbuilding, with local aggradation rate playing a major role in its formation. The local aggradation rate as a controlling factor is viewed cautiously since a high aggradation rate above a salt diapir results in a slower salt rise rate while a high aggradation rate above source layer increases salt supply to diapirs and hence a higher salt rise rate (Jackson and Hudec 2017). This differential loading on local scale may be in turn be controlled by geometry of surrounding salt structures. Relatively shorter basal flap folds are interpreted adjacent to shortened diapirs in the distal early stage contraction province (refer to section 4). Shorter megaflaps show thinner stratal thicknesses and are associated with early onset of high syn-kinematic subsidence.

Shorter flap folds therefore form under relatively shorter time scales or higher regional contraction rates [see (Rowan et al (2016)].

Depositional and structural events in contractional, down-building minibasins

Stratal depositional patterns allowed for interpretations of intermittent syn-kinematic events demonstrated in halokinetic wheeler diagrams (section 5) and structural restorations of minibasin profiles (section 6). Ponding events result in onlaps, while surface erosion events result in angular truncations. Periods of onlap creation/ponding and erosional truncations relative to salt rise that make up syn-kinematic depositional sequence cycle events are punctuated by structural folding of minibasin flanks. Therefore the depositional and structural components that make up syn-kinematic sequences are ponding, flap folding and erosion, classified under the unique stratal patterns the truncated onlap wedge, onlap wedge and truncated hook sequences which are equivalent in timescales to parasequence sets likewise Composite Halokinetic Sequences by Giles & Rowan (2012). The depositional and structural components that make up syn-kinematic sequences are:

1. Ponding – folding – ponding – erosion: These make up syn-kinematic events within the truncated onlap wedge sequence.
2. Ponding – folding – erosion: These form syn-kinematic events within the onlap wedge sequence and
3. Folding – erosion: These make up syn-kinematic events within the truncated hook sequence.

Syn-kinematic events within minibasin sequence packages involving periods of ponding, flap folding and erosion result from significant changes in relative rates of local salt rise and local sedimentation. Influences of relative rates of salt rise and sedimentation have in previous studies been affiliated with geometrical configurations adjacent to salt structures [see Giles and Lawton (2002) and Kernen et al (2012)]. Stratal depocentre shifts or migrating depocentres (Hudec et al. 2009) appear as overall minibasin rotation and are influenced by the preferential flexural drag caused by local differential growth rates of bounding diapirs (Hudec and Jackson 2007; Hudec et al. 2009; Jackson and Hudec 2017) or as a direct response to regional contraction (Duffy et al. 2017).

Flanks of faster growing diapir become the focus of accommodation dictating stratigraphic depocentre axis. P5 diapir-minibasin profile (section 5) showing a highly skewed trajectory of overall minibasin axis towards the P5 diapir is the best case example in this study and in line with concepts of rim or peripheral synclines (Brandes et al. 2012). i.e. A shift from salt-floored downbuilding (Hudec et al. 2009; Vendeville 2002) to peripheral sinks is a critical cue to changes in controlling factors during minibasin evolution. Such changes in controlling factors may be 1) depletion and welding of autochthonous layer (Ferrer et al. 2014; Heidari et al. 2016; Jackson et al. 2010), indicated here in halo-kinematic wheeler diagrams, increased salt rise rate resulting from increased contraction rates may affect salt shapes creating peripheral accommodation (Brun and Fort 2004; Letouzey et al. 1995; Massimi et al. 2007), in such a case, syn-kinematic packages show thickening as opposed to thinning [see (Giles et al. 2004; Giles and Rowan 2012)] towards faster growing diapir.

8. Conclusion

Minibasin sequence divisions are defined by internal stratal depositional patterns and external structural geometries. This is necessary to establish more robust definitions and classifications of minibasin sequences. This study provides an approach to improved kinematic analysis of diapir and minibasin evolution and interaction with depositional systems at local scale. Minibasin sequences consist of pre-kinematic layer, pre-diapiric and halo-kinematic sequence packages. Structural drags of the minibasin sequences initiates and evolve from the onset of vertical salt kinesis and therefore interplay in the sequence cycles of the pre-diapiric and kinematic sequences. The syn-kinematic sequence cycle of events include depositional and structural components ponding, flap folding and erosion.

9. ACKNOWLEDGEMENTS

We are especially grateful to TGS for providing the seismic data used in this study. At TGS, we are particularly thankful to Neil Hodgson for detailed review of this work and for granting the permission to publish. We address our gratitude to IHS Markit for authorising the use of Kingdom: Seismic and geological interpretation software as part of the Royal Holloway academic licence agreement. We extend our thanks to Ian Watkinson and Peter Burgess (former) at Royal Holloway, Earth Sciences department for invaluable discussions on sequence-stratigraphic interpretations that inspired the near diapir scale wheeler diagrams in this study. Special thanks to Mark Rowan for stimulating discussions on Halokinetic Sequence Stratigraphy aspects of this work. Finally we like to thank our financial sponsors Petroleum Technical Development Fund (PTDF), Nigeria.

10. References

Adam, J., Ge, Z. & Sanchez, M. 2012. Salt-structural styles and kinematic evolution of the Jequitinhonha deepwater fold belt, central Brazil passive margin. Marine and Petroleum Geology, **37**, 101-120, doi: https://doi.org/10.1016/j.marpetgeo.2012.04.010.

Adam, J., Grujic, D. & Ings, S. 2005. 4-D Physical Modeling of Tectonics and Basin Migration during Salt Mobilization at Passive Margins. *2006 AAPG Annual Convention*, Calgary.

Adam, J., Krezsek, C. & Grujic, D. 2006. Thin-skinned extension, salt dynamics and deformation in dynamic depositional systems at passive margins. *8th SEGJ International Symposium Conference Proceedings*,, Kyoto, Japan, 6.

Adam, J. & Salt Dynamics Group. 2008. 4D Physical Simulation of Basin-Scale Salt Tectonic Processes and Coupled Depositional Systems from the Rift Basin to Modern Continental Margin. Touch Briefings - Exploration & Production Oil&Gas Review, **6**, 94-97.

Andrie, J.R., Giles, K.a., Lawton, T.F. & Rowan, M.G. 2012. Halokinetic-sequence stratigraphy, fluvial sedimentology and structural geometry of the Eocene Carroza Formation along La Popa salt weld, La Popa Basin, Mexico. Geological Society, London, Special Publications, **363**, 59-79, doi: 10.1144/SP363.4.

Aschoff, J.L. & Giles, K.A. 2005. Salt diapir-influenced, shallow-marine sediment dispersal patterns: Insights from outcrop analogs. AAPG Bulletin, **89**, 447-469.

Bache, F., Gargani, J., Suc, J.-P., Gorini, C., Rabineau, M., Popescu, S.-M., Leroux, E., Couto, D.D., Jouannic, G., Rubino, J.-L., Olivet, J.-L., Clauzon, G., Dos Reis, A.T. & Aslanian, D. 2015. Messinian evaporite deposition during sea level rise in the Gulf of Lions (Western Mediterranean). Marine and Petroleum Geology, **66**, 262-277, doi: 10.1016/j.marpetgeo.2014.12.013.

Bache, F., Olivet, J.L., Gorini, C., Rabineau, M., Baztan, J., Aslanian, D. & Suc, J.-P. 2009. Messinian erosional and salinity crises: View from the Provence Basin (Gulf of Lions, Western Mediterranean). Earth and Planetary Science Letters, **286**, 139-157, doi: 10.1016/j.epsl.2009.06.021.

Banham, S., G. & Mountney, N., P. 2013. Evolution of fluvial systems in salt-walled mini- basins a review and new insights. Sedimentary Geology, **296**, 142-166.

Bonnel, C., Dennielou, B., Droz, L., Mulder, T. & Berné, S. 2005. Architecture and depositional pattern of the Rhône Neofan and recent gravity activity in the Gulf of Lions (western Mediterranean). Marine and Petroleum Geology, **22**, 827-843, doi: 10.1016/j.marpetgeo.2005.03.003.

Brandes, C., Pollok, L., Schmidt, C., Wilde, V. & Winsemann, J. 2012. Basin modelling of a lignite-bearing salt rim syncline: insights into rim syncline evolution and salt diapirism in NW Germany. Basin Research, **24**, 699-716, doi: 10.1111/j.1365-2117.2012.00544.x.

Brun, J.-P. & Fort, X. 2011a. Salt tectonics at passive margins: Geology versus models. Marine and Petroleum Geology, **28**, 1123-1145, doi: 10.1016/j.marpetgeo.2011.03.004.

Brun, J. & Fort, X. 2004. Compressional salt tectonics (Angolan margin). Tectonophysics, **382**, 129-150.

Brun, J.P. & Fort, X. 2011b. Salt tectonics at passive margins: Geology versus models. Marine and Petroleum Geology, **28**, 1123-1145, doi: doi:10.1016/j.marpetgeo.2011.03.004.

Brun, J.P. & Fort, X.T. 2010. The analysis of salt tectonic systems. *GSL-SEPM Conference - Salt Tectonics, Sedimentation, and Prospectivity*, London.

Butler, R.W.H., McClelland, E. & Jones, R.E. 1999. Calibrating the duration and timing of the Messinian salinity crisis in the Mediterranean: linked tectonoclimatic signals in thrust-top basins of Sicily. Journal of the Geological Society, London, **156**, 827-835.

Carminati, E., Doglioni, C., Gelabert, B., Panza, G.F., Raykova, R.B. & Roca, E. 2004. Evolution of the Western Mediterranean. Principles of Phanerozoic Regional Geology, 1-29.

dos Reis, A.T., Gorini, C. & Mauffret, A. 2005. Implications of salt–sediment interactions on the architecture of the Gulf of Lions deep-water sedimentary systems—western Mediterranean Sea. Marine and Petroleum Geology, **22**, 713-746, doi: 10.1016/j.marpetgeo.2005.03.006.

Droz, L., dos Reis, a.T., Rabineau, M., Berné, S. & Bellaiche, G. 2006. Quaternary turbidite systems on the northern margins of the Balearic Basin (Western Mediterranean): A synthesis. Geo-Marine Letters, **26**, 347-359, doi: 10.1007/s00367-006-0044-0.

Duffy, O.B., Fernandez, N., Hudec, M.R., Jackson, M.P.A., Burg, G., Dooley, T.P. & Jackson, C.A.L. 2017. Lateral mobility of minibasins during shortening: Insights from the SE Precaspian Basin, Kazakhstan. Journal of Structural Geology, **97**, doi: 10.1016/j.jsg.2017.02.002.

Ferrer, O., Roca, E. & Vendeville, B.C. 2014. The role of salt layers in the hangingwall deformation of kinked-planar extensional faults: Insights from 3D analogue models and comparison with the Parentis Basin. Tectonophysics, **636**, 338-350, doi: http://dx.doi.org/10.1016/j.tecto.2014.09.013.

Gemmer, L., Ings, S., Medvedev, S. & Beaumont, C. 2004. Salt tectonics driven by differential sediment loading Stability analysis and finite-element experiments.

Giles, K.A. & Lawton, T.F. 2002. Halokinetic Sequence Stratigraphy Adjacent to the El Papalote Diapir, Northeastern Mexico. American Associacion of Petroleum Geologists Bulletin, **86**, 823-840, doi: 10.1306/61eedbac-173e-11d7-8645000102c1865d.

Giles, K.A., Lawton, T.F. & Rowan, M.G. 2004. Summary of Halokinetic Sequence Chacteristics from Outcrop Studies of La Popa Salt Basin, Northeastern Mexico. *24th Bob F. Perkins Research Conference*, Houston, Texas, 625-634.

Giles, K.A. & Rowan, M.G. 2012. Concepts in halokinetic-sequence deformation and stratigraphy. Geological Society, London, Special Publications, **363**, 7-31, doi: 10.1144/sp363.2.

Gottschalk, R.R., Anderson, A.V., Walker, J.D. & Da Silva, J.C. 2004. Modes of contractional salt tectonics in Angola Block 33, Lower Congo Basin, West Africa. *Sediment Interactions and Hydrocarbon Prospectivity, Concepts, Applications and Case Studies for the 21st Century*, SEPM, Houston, TX., 705-734.

Granado, P., Urgeles, R., Sàbat, F., Albert Villanueva, E., Roca, E., Muñoz, J., Mazzuca, N. & Gambini, R. 2016. Geodynamical framework and hydrocarbon plays of a salt giant: the NW Mediterranean Basin. Petroleum Geoscience, **22**, doi: 10.1144/petgeo2015-084.

Gunnell, Y., Zeyen, H. & Calvet, M. 2008. Geophysical evidence of a missing lithospheric root beneath the Eastern Pyrenees: Consequences for post-orogenic uplift and associated geomorphic signatures. Earth and Planetary Science Letters, **276**, 302-313, doi: 10.1016/j.epsl.2008.09.031.

Heidari, M., Nikolinakou, M.A., Hudec, M.R. & Flemings, P.B. 2016. Geomechanical analysis of a welding salt layer and its effects on adjacent sediments. Tectonophysics, **683**, 172-181, doi: 10.1016/j.tecto.2016.06.027.

Hudec, M.R. 2003. Quick-look chart for restoration of salt structures in cross section. Bureau of Economic Geology Publication, EM0009, poster + 10-page booklet.

Hudec, M.R. & Jackson, M.P.A. 2007. Terra infirma: Understanding salt tectonics. Earth-Science Reviews, **82**, 1-28.

Hudec, M.R., Jackson, M.P.A. & Schultz-Ela, D.D. 2009. The paradox of minibasin subsidence into salt: Clues to the evolution of crustal basins. Bulletin of the Geological Society of America, doi: 10.1130/B26275.1.

Ings, S., Beaumont, C. & Gemmer, L. 2004. Numerical Modeling of Salt Tectonics on Passive Continental Margins: Preliminary Assessment of the Effects of Sediment Loading, Buoyancy, Margin Tilt, and Isostasy. *24th Annual GCSSEPM Foundation Bob F. Perkins Research Conference Proceedings*, 38-68.

Jackson, M., Cloos, M., Hudec, M., Steel, R., Sen, M. & Peel, F. 2010. An Analysis of Salt Welding.

Jackson, M.P.A. & Hudec, M.R. 2011. Salt Tectonics: Priciples and Practice

Jackson, M.P.A. & Hudec, M.R. 2017. Salt Tectonics: Principles and Practice. Cambridge University Press.

Kernen, R.A., Giles, K.A., Rowan, M.G., Lawton, T.F. & Hearon, T.E. 2012. Depositional and halokinetic-sequence stratigraphy of the Neoproterozoic Wonoka

Formation adjacent to Patawarta allochthonous salt sheet, Central Flinders Ranges, South Australia. *In*: Archer, S.G., Alsop, G.I., Hartley, A.J., Grant, N.T. & Hodgkinson, R. (eds.) *Salt Tectonics, Sediments and Prospectivity*. Geological Society, 81-105.

Leroux, E., Aslanian, D., Rabineau, M., Moulin, M., Granjeon, D., Gorini, C. & Droz, L. 2015. Sedimentary markers in the Provençal Basin (western Mediterranean): a window into deep geodynamic processes. Terra Nova, **27**, 122-129, doi: 10.1111/ter.12139.

Letouzey, J., Colletta, B., Vially, R. & Chermette, J.C. 1995. Evolution of Salt-Related Structures in Compressional Settings. *In*: Jackson, M.P.A., Roberts, D.G. & Snelson, S. (eds.) *Salt tectonics: a global perspective: AAPG Memoir*. AAPG, 41-60.

Madof, A.S., Christie-Blick, N. & Anders, M.H. 2009. Stratigraphic controls on a salt-withdrawal intraslope minibasin, north-central Green Canyon, Gulf of Mexico: Implications for misinterpreting sea level change. AAPG Bulletin, **93**, 535-561, doi: 10.1306/12220808082.

Maillard, A., Gaullier, V., Vendeville, B.C. & Odonne, F. 2003. Influence of differential compaction above basement steps on salt tectonics in the Ligurian-Provencal Basin, Northwest Mediterranean. Marine and Petroleum Geology, **20**, 13-27.

Mannie, A.S., Jackson, C.A.L. & Hampson, G.J. 2014. Shallow-marine reservoir development in extensional diaper-collapse minibasins: An integrated subsurface case study from the Upper Jurassic of the Cod terrace, Norwegian North Sea. AAPG Bulletin, **98**, 2019-2055, doi: 10.1306/03201413161.

Maria A. Nikolinakou, M.H., Michael R. Hudec, & Flemings, P.B. 2017. Initiation and growth of salt diapirs in tectonically stable settings: Upbuilding and megaflaps. AAPG Bulletin, **101**, 887-905, doi: 10.1306/09021615245.

Massimi, P., Quarteroni, A., Saleri, F. & Scrofani, G. 2007. Modeling of salt tectonics. Computer Methods in Applied Mechanics and Engineering, **197**, 281-293.

Mianaekere, V. & Adam, J. 2020. 'Halo-kinematic' sequence stratigraphic analysis adjacent to salt diapirs in the deepwater contractional province, Liguro-Provencal Basin, western mediterranean. Marine and Petroleum Geology, 104258, doi: https://doi.org/10.1016/j.marpetgeo.2020.104258.

Nikolinakou, M.A., Heidari, M., Hudec, M.R. & Flemings, P.B. 2017. Initiation and growth of salt diapirs in tectonically stable settings: Upbuilding and megaflaps. AAPG Bulletin, **101**, 887-905, doi: 10.1306/09021615245.

Peel, F.J. 2014. How do salt withdrawal minibasins form? Insights from forward modelling, and implications for hydrocarbon migration. Tectonophysics, **630**, 222-235, doi: 10.1016/j.tecto.2014.05.027.

Ribes, C., Kergaravat, C., Bonnel, C., Crumeyrolle, P., Callot, J.-P., Poisson, A., Temiz, H. & Ringenbach, J.-C. 2015. Fluvial sedimentation in a salt-controlled mini-basin: stratal patterns and facies assemblages, Sivas Basin, Turkey. Sedimentology, **62**, 1513-1545, doi: 10.1111/sed.12195.

Roberts, D.G. & christoffersen, T. 2013. The West Mediterranean Salt Basin – A Future Petroleum Producing Province.

Rouchy, J.M. & Caruso, A. 2006. The Messinian salinity crisis in the Mediterranean basin: A reassessment of the data and an integrated scenario. Sedimentary Geology, **188**, 35-67.

Rowan, M., Peel, F. & Vendeville, B. 2004. Gravity-driven fold belts on passive margins. *In*: McClay, K.R. (ed.) *Thrust tectonics and hydrocarbon systems*. AAPG Memoir, 157–182.

Rowan, M.G., Giles, K.a., Hearon IV, T.E. & Fiduk, J.C. 2016. Megaflaps adjacent to salt diapirs. AAPG Bulletin, **100**, 1723-1747, doi: 10.1306/05241616009.

Rowan, M.G., Lawton, T.F. & Giles, K.A. 2012a. Anatomy of an exposed vertical salt weld and flanking strata, La Popa Basin, Mexico. Geological Society, London, Special Publications, **363**, 33-57, doi: 10.1144/sp363.3.

Rowan, M.G., Lawton, T.F., Giles, K.A. & Ratliff, R.A. 2003. Near-salt deformation in La Popa basin, Mexico, and the northern Gulf of Mexico: A general model for passive diapirism. AAPG Bulletin, **87**, 733-756.

Rowan, M.G., Peel, F.J., Vendeville, B.C. & Gaullier, V. 2012b. Salt tectonics at passive margins: Geology versus models – Discussion. Marine and Petroleum Geology, doi: 10.1016/j.marpetgeo.2012.04.007.

Rowan, M.G. & Ratliff, R.A. 2012. Cross-section restoration of salt-related deformation: Best practices and potential pitfalls. Journal of Structural Geology, doi: 10.1016/j.jsg.2011.12.012.

Saura, E., Ardèvol i Oró, L., Teixell, A. & Vergés, J. 2016. Rising and falling diapirs, shifting depocenters, and flap overturning in the Cretaceous Sopeira and Sant Gervàs subbasins (Ribagorça Basin, southern Pyrenees). Tectonics, **35**, 638-662, doi: 10.1002/2015tc004001.

Schreurs, G., Haenni, R., Panien, M. & Vock, P. 2003. Analysis of analogue models by helical X-ray computed tomography. Geological Society Special Publications, **215**, 213-223.

Schultz-Ela, D.D. 2003. Origin of drag folds bordering salt diapirs. AAPG Bulletin, **87**, 757-780, doi: 10.1306/12200201093.

Schultz-Ela, D.D., Jackson, M.P.A. & Vendeville, B.C. 1993. Mechanics of active salt diapirism. Tecfonophysics, **228**, 215-312.

Storetvedt, K.M. 1973. Genesis of West Mediterranean basins. Earth and Planetary Science Letters., **21**, 22-28, doi: 10.1016/0012-821X(73)90221-5.

Tari, G., Molnar, J. & Ashton, P. 2003. Examples of salt tectonics from West Africa: a comparative approach. *In*: Arthur, T.J., MacGregor, D.S. & Cameron, N. (eds.)

Petroleum Geology of Africa: New Themes and Developing Technologies. Geological Society of London, Special Publications, 85-104.

Vendeville, B. 2002. A new Interpretation of Trusheim's Classic Model of Salt-Diapir Growth. Gulf Coast Association of Geological Societies Transactions, **52**.

Vendeville, B.C., Jackson, M.P.A. & Anonymous. 1990. Physical modeling of the growth of extensional and contractional salt tongues on continental slopes. AAPG Bulletin, **74**, 784.

Waltham, D. 1997. Why does salt start to move? *Tectonophysics*, 117-128.

Wheeler, H.E. 1958. Time-stratigraphy. AAPG Bulletin, **42**, 1047-1063.